Calibration of a soft secondary vertex tagger using proton-proton collisions at $\sqrt{s} = 13$ TeV with the ATLAS detector

G. Aad *et al.*[*]
(ATLAS Collaboration)

(Received 7 May 2024; accepted 26 June 2024; published 19 August 2024)

Several processes studied by the ATLAS experiment at the Large Hadron Collider produce low-momentum b-flavored hadrons in the final state. This paper describes the calibration of a dedicated tagging algorithm that identifies b-flavored hadrons outside of hadronic jets by reconstructing the soft secondary vertices originating from their decays. The calibration is based on a proton-proton collision dataset at a center-of-mass energy of 13 TeV corresponding to an integrated luminosity of 140 fb^{-1}. Scale factors used to correct the algorithm's performance in simulated events are extracted for the b-tagging efficiency and the mistag rate of the algorithm using a data sample enriched in $t\bar{t}$ events. Several orthogonal measurement regions are defined, binned as a function of the multiplicities of soft secondary vertices and jets containing a b-flavored hadron in the event. The mistag rate scale factors are estimated separately for events with low and high average numbers of interactions per bunch crossing. The results, which are derived from events with low missing transverse momentum, are successfully validated in a phase space characterized by high missing transverse momentum and therefore are applicable to new physics searches carried out in either phase space regime.

DOI: 10.1103/PhysRevD.110.032015

I. INTRODUCTION

The accurate reconstruction and identification of particles traversing the ATLAS detector is a fundamental aspect of the experiment's successful physics program. This includes the identification of jets that contain a b-flavored hadron (B-hadron in the following), referred to as b-jets, which is crucial for enabling precise measurements and discoveries of processes involving heavy particles that decay into b-quarks. The distinctive decay patterns and long lifetimes of B-hadrons, as well as the fragmentation properties of b-quarks, provide a powerful handle for distinguishing b-jets from jets originating from lighter quarks or gluons. The ATLAS Collaboration has developed various algorithms to identify b-jets, referred to as b-tagging algorithms [1–3], which are essential for analyzing the data recorded at the Large Hadron Collider (LHC).

The use of jets as a starting point for b-tagging imposes constraints on the energy of both the B-hadron and the surrounding hadronic activity. Standard b-tagging techniques in ATLAS are applicable to jets with transverse momenta (p_{T}) of at least 20 GeV. However, many scenarios beyond the Standard Model (SM) predict final states with B-hadrons at lower p_{T}, such that their identification would greatly improve the associated analysis sensitivity.

One class of processes that could give rise to low-p_{T} B-hadrons is the production of the supersymmetric (SUSY) partners of third generation quarks (top and bottom squarks). In particular, compressed-SUSY scenarios [4–9], where either the top or the bottom squark is nearly mass degenerate with the lightest SUSY particle, are favored in scenarios of electroweak baryogenesis. The low p_{T} of the squark decay products makes such scenarios difficult to separate from background. The p_{T} spectrum of the final-state particles in such events may peak as low as 4 GeV depending on the mass compression.

Other examples of searches for physics beyond the SM that may benefit from low-p_{T} B-hadron identification are searches for exotic decays of the Higgs boson [10] into new light pseudoscalar particles. Such processes can involve the production of up to six b-quarks in the final state [11]. Depending on the relative mass difference between the new pseudoscalar states and the Higgs boson, the p_{T} spectrum of the lowest-p_{T} b-quarks can peak as low as 10 GeV. The ability to identify such low-p_{T} b-quarks is crucial for the analysis performance in discriminating the signal from the SM background.

The ATLAS Collaboration has developed algorithms tagging low-p_{T} B-hadrons arising in compressed bottom squark [12] and top squark [13] searches, with b-quarks in the final state. The CMS Collaboration has also

[*]Full author list given at the end of the article.

successfully implemented similar techniques in the context of compressed-SUSY scenarios [14]. This paper focuses on the calibration of the track-cluster-based low-p_{T} vertex tagger (TC-LVT). This algorithm is based on the reconstruction of secondary vertices outside of jets identified by traditional clustering algorithms and targets the reconstruction of B-hadrons with p_{T} between 5 and 20 GeV.

A data sample containing predominantly top-antitop-quark ($t\bar{t}$) events is selected, where both top quarks decay into a W boson and a b-quark, followed by a subsequent decay of each W boson into either an electron or a muon and a neutrino.

This paper is organized as follows. In Sec. II the ATLAS detector is described. The data and simulated samples used in the calibration are described in Sec. III. Section IV summarizes the reconstruction of tracks, electrons, muons, and jets, followed by a description of the TC-LVT algorithm in Sec. V. Section VI describes the event selection and calibration method, systematic uncertainties, and results. The conclusions are given in Sec. VII.

II. THE ATLAS DETECTOR

The ATLAS detector [15] at the LHC covers nearly the entire solid angle around the collision point.[1] It consists of an inner tracking detector surrounded by a thin superconducting solenoid, electromagnetic and hadronic calorimeters, and a muon spectrometer incorporating three large superconducting air-core toroidal magnets.

The inner-detector system is immersed in a 2 T axial magnetic field and provides charged-particle tracking in the range $|\eta| < 2.5$. The high-granularity silicon pixel detector covers the vertex region and typically provides four measurements per track, the first hit generally being in the insertable B-layer installed before Run 2 [16,17]. It is followed by the semiconductor tracker (SCT), which usually provides eight measurements per track. These silicon detectors are complemented by the transition radiation tracker (TRT), which enables radially extended track reconstruction up to $|\eta| = 2.0$. The TRT also provides electron identification information based on the fraction of hits (typically 30 in total) above a higher energy-deposit threshold corresponding to transition radiation.

The calorimeter system covers the pseudorapidity range $|\eta| < 4.9$. Within the region $|\eta| < 3.2$, electromagnetic calorimetry is provided by barrel and end cap high-granularity lead/liquid-argon (LAr) calorimeters, with an additional thin LAr presampler covering $|\eta| < 1.8$ to correct for energy loss in material upstream of the calorimeters. Hadronic calorimetry is provided by the steel/scintillator-tile calorimeter, segmented into three barrel structures within $|\eta| < 1.7$, and two copper/LAr hadronic end cap calorimeters. The solid angle coverage is completed with forward copper/LAr and tungsten/LAr calorimeter modules optimized for electromagnetic and hadronic energy measurements, respectively.

The muon spectrometer comprises separate trigger and high-precision tracking chambers measuring the deflection of muons in a magnetic field generated by the superconducting air-core toroidal magnets. The field integral of the toroids ranges between 2.0 and 6 T m across most of the detector. Three layers of precision chambers, each consisting of layers of monitored drift tubes, cover the region $|\eta| < 2.7$, complemented by cathode-strip chambers in the forward region, where the background is highest. The muon trigger system covers the range $|\eta| < 2.4$ with resistive-plate chambers in the barrel, and thin-gap chambers in the end cap regions.

The luminosity is measured mainly by the LUCID-2 [18] detector that records Cherenkov light produced in the quartz windows of photomultipliers located close to the beam pipe.

Events are selected by the first-level trigger system implemented in custom hardware, followed by selections made by algorithms implemented in software in the high-level trigger [19]. The first-level trigger accepts events from the 40 MHz bunch crossings at a rate below 100 kHz, which the high-level trigger further reduces in order to record complete events to disk at about 1 kHz.

A software suite [20] is used in data simulation, in the reconstruction and analysis of real and simulated data, in detector operations, and in the trigger and data acquisition systems of the experiment.

III. DATA AND SIMULATED EVENT SAMPLES

The results presented in this paper are based on data collected by the ATLAS experiment between 2015 and 2018 during Run 2 of the LHC. The dataset corresponds to an integrated luminosity of 140 fb^{-1} [18,21] of pp collisions at a center-of-mass energy of 13 TeV. Events were selected at trigger level based on the presence of at least one electron [22] or muon [23]. These single-lepton triggers were configured with p_{T} thresholds ranging from 20 to 26 GeV, depending on the lepton flavor and data-taking period. Every detector subsystem must have been in operation during data collection. Moreover, stringent data quality criteria were applied to ensure the reliability of the data [24].

Simulated samples of SM processes are based on Monte Carlo (MC) techniques, and the main contributing samples are described in the following. All simulated samples are processed through the ATLAS simulation

[1] ATLAS uses a right-handed coordinate system with its origin at the nominal interaction point (IP) in the center of the detector and the z axis along the beam pipe. The x axis points from the IP to the center of the LHC ring, and the y axis points upward. Polar coordinates (r, ϕ) are used in the transverse plane, ϕ being the azimuthal angle around the z axis. The pseudorapidity is defined in terms of the polar angle θ as $\eta = -\ln\tan(\theta/2)$. Angular distance is measured in units of $\Delta R \equiv \sqrt{(\Delta\eta)^2 + (\Delta\phi)^2}$.

infrastructure [25] including a detailed model of the ATLAS detector based on Geant4 [26].

The effect of multiple interactions in the same and neighboring bunch crossings (pileup) are modeled by overlaying the simulated hard-scattering event with inelastic pp events generated with Pythia 8.186 [27] using the NNPDF2.3LO [28] set of parton distribution functions (PDFs) and the A3 set of tuned parameters [29]. The MC events are weighted to reproduce the distribution of the average number of interactions per bunch crossing (μ) observed in the data, where the μ value in data is rescaled by a factor of 1.03 ± 0.04 to improve agreement between data and simulation in the visible inelastic proton-proton cross section [30]. A further correction to the distribution is derived in the sample selected by this analysis such that the μ distribution in simulated events matches the one in data for the calibration measurement.

The analysis presented in this paper is designed to select $t\bar{t}$ events where each of the top quarks decays leptonically, hence the modeling of this SM process is particularly important. A suite of MC samples with different accuracy in the matrix element (ME) and different models for the parton shower (PS) are used for the $t\bar{t}$ process. The baseline $t\bar{t}$ simulated sample was produced using the POWHEG BOX [31] v2 generator with a ME at next-to-leading order (NLO) in quantum chromodynamics (QCD) in the five-flavor scheme, and interfaced to Pythia 8.230 [32] with the A14 set of tuned parameters [33] to model PS, hadronization, and the underlying event. The PDF sets NNPDF3.0NNLO and NNPDF2.3LO [28,34] were used in the ME-PS matching, respectively. The h_{damp} parameter, which controls the matching in POWHEG and effectively regulates the high-p_{T} radiation against which the $t\bar{t}$ system recoils, was set to $1.5m_t$ [35]. The functional form of the renormalization and factorization scales was set to the default scale ($\sqrt{m_t^2 + p_{\text{T},t}^2}$).

Alternative $t\bar{t}$ simulation samples were generated using POWHEG BOX v2 interfaced to Herwig7.04 [36] with the H7-UE-MMHT set of tuned parameters. Uncertainties related to initial- (ISR) and final-state radiation (FSR) are estimated by reweighting the baseline $t\bar{t}$ events such that initial (final) parton shower radiation [35] is increased or reduced and by using an alternative POWHEG BOX v2 + Pythia 8.230 sample with h_{damp} set to $3m_t$ and the parameter variation group Var3 (described in Ref. [35]) increased, leading to increased ISR.

Samples with $t\bar{t} + b\bar{b}$ MEs were produced at NLO QCD accuracy with the POWHEG BOX RES [37] generator and OpenLoops [38–40], using a prerelease of the implementation of this process in POWHEG BOX RES provided by the authors [41], with the NNPDF3.0NLO nf4 [34] PDF set. It was interfaced with Pythia 8.240 [32], using the A14 set of tuned parameters [33] and the NNPDF2.3LO PDF set. The four-flavor scheme was used with the b-quark mass set to 4.95 GeV. The factorization scale was set to $0.5 \times \Sigma_{i=t,\bar{t},b,\bar{b},j} m_{\text{T},i}$, the renormalization scale was set to $\sqrt[4]{m_{\text{T},t} \cdot m_{\text{T},\bar{t}} \cdot m_{\text{T},b} \cdot m_{\text{T},\bar{b}}}$, and the h_{damp} parameter was set to $0.5 \times \Sigma_{i=t,\bar{t},b,\bar{b}} m_{\text{T},i}$. Events containing two B-hadrons produced in the decay of the two top quarks and either one or two additional B-hadrons with $p_{\text{T}} > 5$ GeV and matched to a particle jet are vetoed in the nominal $t\bar{t}$ sample and taken from the $t\bar{t} + b\bar{b}$ sample. Events with an additional c-flavored hadron with $p_{\text{T}} > 5$ GeV and matched to a particle jet undergo the same procedure.

Additional processes entering the analysis selection arise from the production of a single top quark, either through the associated production with a W boson (tW) or in t-channel and s-channel production. These contributions were modeled by the POWHEG BOX v2 [42–44] generator with a ME at NLO. For t-channel production, events were generated in the four-flavor scheme with the NNPDF3.0NLO nf4 PDF set, and the functional form of the renormalization and factorization scale was set to $\sqrt{m_b^2 + p_{\text{T},b}^2}$ following the recommendation of Ref. [42]. For s-channel and tW production, events were generated in the five-flavor scheme with the NNPDF3.0NLO PDF set, and the functional form of the renormalization and factorization scale was set to the default scale, which is equal to the top-quark mass. For tW production, the diagram removal scheme [45] was employed to treat the interference with $t\bar{t}$ production [35]. To evaluate the impact of the PS and hadronization model, the same events produced for the nominal POWHEG BOX + Pythia8 samples were used, but they were showered with Herwig7.04. To assess the uncertainty due to the choice of the matching scheme, the nominal samples are compared with samples generated with the MadGraph5_aMC@NLO v2.6.2 [46] generator at NLO in QCD, in the four-flavor scheme for t-channel production, and in the five-flavor scheme for s-channel and tW production. For t-channel production (respectively, s-channel, tW production), the NNPDF3.0NLO PDF set is used.

To evaluate the effect of employing the diagram subtraction scheme instead of the diagram removal scheme [44,45] for tW events, alternative samples were produced, where the diagram subtraction scheme was used. All single-top-quark samples were showered with Pythia 8.230, unless otherwise stated for studies assessing systematic uncertainties.

Additional small contributions are expected from Z + jets processes, which were modeled with the Sherpa 2.2.1 [47] generator providing NLO MEs for up to two partons in addition to the Z boson and leading-order MEs for up to four partons calculated with the Comix [48] and OpenLoops libraries. These samples were matched with the Sherpa parton shower [49] using the MEPS@NLO prescription [50–53]. The NNPDF3.0NNLO set of PDFs [34] was used.

Several rare processes such as $t\bar{t}V$ (where V is either a W or Z boson), $t\bar{t}H$, four-top-quark production and VV are

considered as well, however, they have a negligible contribution in the phase space considered.

The EvtGen 1.6.0 program [54] was employed to simulate the decay of b- and c-flavored hadrons in all samples except those generated using Sherpa, for which the default configuration recommended by the Sherpa authors was used.

IV. OBJECT RECONSTRUCTION

Tracks are reconstructed from hits inside the inner tracking detector [55,56]. In addition to acceptance criteria of $|\eta| < 2.5$ and $p_{\mathrm{T}} > 500$ MeV, the tracks must satisfy a set of quality criteria defined by the *Loose* working point in Ref. [55]. Tracks should have at least seven hits in the silicon detectors with no more than one detector module shared with other tracks, no more than one missing hit in the pixel detector, and no more than two missing hits in the SCT detector. Events are required to contain at least one vertex with two or more associated tracks, and the vertex with the highest p_{T}^2 sum of the associated tracks is taken as the primary vertex (PV) [57]. Transverse and longitudinal impact parameters, d_0 and z_0, are used to identify tracks that originate at a certain displacement from the PV (e.g. B-hadron decay products). The transverse impact parameter, d_0, is the point of closest approach to the measured beam line position; and z_0, required to satisfy $|z_0 \sin\theta| < 3$ mm, is the difference between the longitudinal position of the track along the beam line at the point where d_0 is measured and the longitudinal position of the primary vertex [58]. The latter requirement reduces the contamination from pileup, secondary, and fake tracks. The collection of tracks satisfying the criteria stated above is used as input to the TC-LVT tagger for the reconstruction of soft secondary vertex (SSV) candidates. The complete set of requirements for tracks used for standard high-p_{T} b-tagging algorithms are described in Ref. [3].

Electron candidates are reconstructed from energy deposits (clusters) in the electromagnetic calorimeter associated with reconstructed tracks in the inner detector [59]. Candidates that satisfy $p_{\mathrm{T}} > 10$ GeV and $|\eta| < 2.47$ are selected, excluding the calorimeter transition region $1.37 < |\eta| < 1.52$. Electrons must satisfy the *Tight* likelihood-based identification criterion and are required to satisfy the criteria of the *PLVLoose* working point of the "prompt lepton tagger" [60], a multivariate isolation discriminant used to reject nonprompt leptons from heavy-flavor decays. They are further required to have $|z_0 \sin\theta| < 0.5$ mm and $|d_0/\sigma(d_0)| < 5$, where the longitudinal and transverse impact parameters d_0 and z_0 are computed relative to the primary vertex and $\sigma(d_0)$ is the resolution of the track transverse impact parameter d_0. It is computed using an iterative Gaussian fit performed on the core of the impact parameter distribution [61].

Muon candidates are reconstructed from track segments in the various layers of the muon spectrometer, and matched with tracks from the inner detector [62]. The final muon candidates are refitted using the complete track information from both detector systems, and required to satisfy $p_{\mathrm{T}} > 10$ GeV and $|\eta| < 2.5$. Muons are required to satisfy the *Medium* quality requirements and to satisfy the isolation criteria of the *PLVLoose* working point of the prompt lepton tagger. The absolute value of the muon d_0 significance must be less than 3, and the value of $|z_0 \sin\theta|$ must be less than 0.5 mm.

Jets are reconstructed by clustering particle-flow objects [63] with the anti-k_t algorithm [64,65] with a radius parameter of $R = 0.4$ and a four-momentum recombination scheme. The jet energy is corrected to the particle level by the application of a jet energy scale calibration derived from pp collision data and simulation at $\sqrt{s} = 13$ TeV [66]. Baseline jets are required to have $p_{\mathrm{T}} > 20$ GeV and $|\eta| < 2.5$. They are also required to satisfy a *Tight* pileup rejection criterion based on the jet vertex tagger (JVT) score [67]: for jet $p_{\mathrm{T}} \in [20, 60]$ GeV and $|\eta| < 2.4$, the JVT score must be higher than 0.5.

The identification of b-jets with $p_{\mathrm{T}} > 20$ GeV is done using the DL1r algorithm [3], a high-level tagger based on a deep neural network (NN). The NN is trained on simulated $t\bar{t}$ and Z' events and uses the results of specialized low-level taggers, based on track impact parameters, secondary vertices, and decay topologies, to obtain the probability for each jet to be a b-, c-, or light-jet. In this measurement the 85% working point is used, corresponding to an 85% efficiency to correctly tag a b-jet in simulated $t\bar{t}$ events.

To avoid double counting of the objects used in the analysis, special care is taken to remove any potential overlap. This procedure is based on two object distances defined by $\Delta R_y = \sqrt{(\Delta y)^2 + (\Delta\phi)^2}$, where y is the rapidity and ϕ the azimuthal angle of each object. The removal is carried out systematically starting with electrons, where the closest jet within $\Delta R_y = 0.2$ of a selected electron is removed. If the nearest jet surviving that selection is within $\Delta R_y = 0.4$ of the electron, the electron is discarded. Muons are removed if they are separated from the nearest jet by $\Delta R_y < 0.4$, which reduces the background from heavy-flavor decays inside jets. However, the muon is kept and the jet removed instead if fewer than three tracks are associated with the jet. This criterion avoids inefficiency for the selection of high-energy muons undergoing significant energy loss in the calorimeter.

The missing transverse momentum, with magnitude $E_{\mathrm{T}}^{\mathrm{miss}}$, is defined as the negative vector sum of the transverse momenta of all selected and calibrated electrons, muons, and jets in the event, with an extra term added to account for energy in the event that is not associated with any of these objects [68].

V. SOFT SECONDARY VERTEX ALGORITHM DEFINITION AND PERFORMANCE

A. TC-LVT algorithm description

The TC-LVT algorithm is based on vertexing techniques first developed in the context of standard b-tagging, which

TABLE I. Selection criteria applied to the objects in the vertex reconstruction of the TC-LVT algorithm.

Seed track	Cluster tracks	Vertex
$\lvert d_0/\sigma(d_0)\rvert > 0.5$	$\lvert d_0/\sigma(d_0)\rvert > 1.5$	$600\,\text{MeV} < m_{\text{vtx}} < 6\,\text{GeV}$
$p_{\text{T}} > 1.5$ GeV	$\Delta R_{\text{seed}}^{\text{track}} < 0.75$	$p_{\text{T}}^{\text{vtx}} > 3$ GeV
	$d_{\text{seed}}^{\text{track}} < 0.25$ mm	

are retuned and applied outside hadronic jets. It aims to identify B-hadrons outside hadronic jets by reconstructing displaced secondary vertices. The key ingredients of the algorithm are seed tracks, cluster tracks (which are inputs to track clusters in the following), and reconstructed vertices as defined by the selection criteria summarized in Table I. These criteria define the *Loose* working point and were optimized to maximize the efficiency of the algorithm.

As a first step a set of *seed tracks* is extracted. The seed tracks are characterized by a high transverse momentum of $p_{\text{T}} > 1.5$ GeV and $|d_0/\sigma(d_0)| > 0.5$. Tracks that are also matched to a track-jet [69] with $p_{\text{T}} > 20$ GeV are not considered. The list of seed tracks is ordered in decreasing p_{T}. Clusters of tracks are built around these seed tracks by adding additional high-displacement tracks ($|d_0/\sigma(d_0)| > 1.5$) within an angular distance to the seed track of $\Delta R_{\text{seed}}^{\text{track}} < 0.75$ and within a track-to-track distance of closest approach $d_{\text{seed}}^{\text{track}} < 0.25$ mm. Once tracks are associated with a cluster, they are not considered further for other clusters.

The next step of the algorithm is the vertexing process, which is accomplished using the single secondary vertex finding (SSVF) algorithm [70]. For clarity, in the following the main features of this algorithm are described and the reader is referred to Ref. [70] for details. For each identified cluster, the SSVF algorithm is executed on all tracks within $\Delta R = 0.4$ from the vector sum of the momenta of all tracks associated with the cluster. First, all the possible pairs of tracks originating from nearby points are combined into two-track vertices. Further requirements are applied to the two-track vertices to reduce the number of fake vertices and material interactions. For example, the tracks associated with the vertex must not have any hits in detector layers at a radius smaller than that of the vertex itself. Two-track vertices located in regions of the detector with large amounts of material are eliminated according to the procedure described in Ref. [70]. Two-track vertices with invariant masses consistent with K_S^0 and Λ^0 decays are identified, and the corresponding tracks are removed if the impact parameter of the reconstructed pair is consistent with the primary vertex. Similarly, two-track vertices with invariant masses below 40 MeV under the e^+e^- hypothesis are excluded to reject photon conversions. Finally, all tracks contributing to the cleaned set of two-track vertices are combined into one list of selected tracks. This track list is supplied to the vertex fitter.

The vertex fitter runs iteratively on all the tracks in the list, trying to fit one secondary vertex from all these tracks. In each iteration the track with the largest χ^2 (track, vertex) of the track-vertex association is removed and the vertex fit is repeated until an acceptable vertex χ^2 (vertex) is found. The mass m_{vtx} of the vertex is defined as the invariant mass of the four-vector sum of the constituent tracks and required to be above 600 MeV and below 6 GeV. The higher threshold is chosen to reject random track crossings while maximizing efficiency for true B-hadron vertices. The lower threshold is optimized to reject the most common light-flavored long-lived hadrons. For similar reasons, the $p_{\text{T}}^{\text{vtx}}$ of the reconstructed vertex is defined as the p_{T} of the four-vector sum of the constituent tracks, and required to be above 3 GeV.

As a last step, if two vertices are found they are merged if their angular distance $\Delta R < 0.3$. This occurs rarely but helps the treatment of secondary or tertiary decays in the same hadron decay chain. The four-vectors of the merged vertices are added and the resulting vertex retains the parameter values, e.g. L_{xy} (the displacement in the transverse plane of the secondary vertex relative to the primary vertex) or $L_{3\text{D}}$ (the significance of the 3D distance relative to the primary vertex), of the merged vertex with smallest L_{xy}.

Objects identified with the TC-LVT algorithm, henceforth referred to as soft secondary vertices or SSVs, are removed if they are within $\Delta R < 0.2$ of a reconstructed lepton or within $\Delta R < 0.6$ of a reconstructed jet.

B. TC-LVT algorithm performance

The performance of the TC-LVT algorithm is investigated using the full set of samples described in Sec. III and applying the event selection described in Sec. VI A. The parameters used in this study are

(i) ε_{ssv}: probability that a true SSV is identified by the TC-LVT tagger, and
(ii) n_f: expected average number of fake SSVs per event.

The *Loose* working point of the TC-LVT algorithm (see Table I) is used, which is designed to maximize the efficiency of the algorithm while achieving the lowest possible fake rate. The classification of true and fake SSVs is done based on a cone-matching requirement between the reconstructed SSV and a simulated B-hadron in acceptance. A B-hadron is considered to be in acceptance if it meets the criteria of $p_{\text{T}} > 2$ GeV, $|\eta| < 2.8$, and $\Delta R_{\text{min}}(B, \text{jet}) > 0.3$, where the latter ensures that the B-hadron is located outside of any reconstructed jet. These acceptance requirements are driven by the ATLAS tracking detector geometry and the typical jet distance parameters used in the jet reconstruction. SSVs fulfilling $\Delta R(B, SSV) < 0.3$ are considered true SSVs, and their event multiplicity is indicated by $\mathcal{N}_{\text{ssv}}$. Unmatched SSVs are considered fake SSVs. SSVs matched to a c-flavored hadron in acceptance are also categorized as true SSVs, as long as the c-flavored hadron

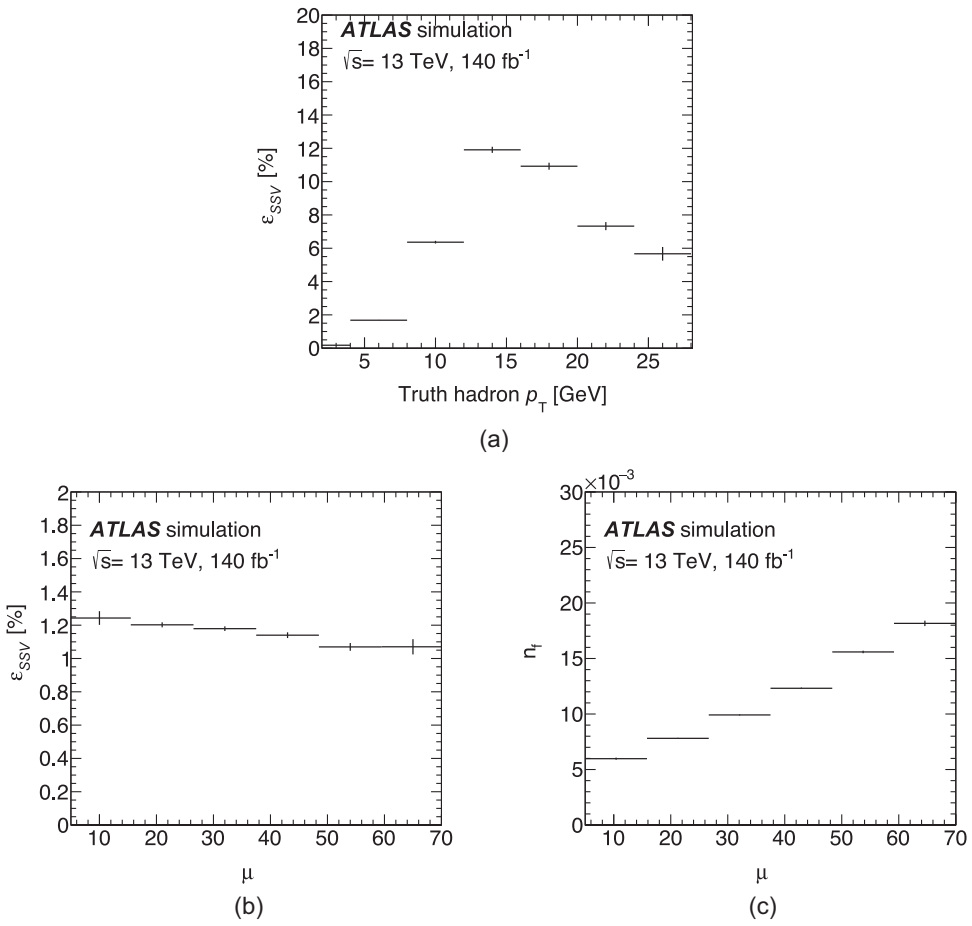

FIG. 1. TC-LVT efficiency to reconstruct true SSVs as a function of (a) truth hadron p_{T} and (b) average number of interactions per bunch crossing, μ. (c) Average number of fake SSVs per event, n_f, as a function of μ. A B-hadron is considered to be in acceptance if it meets the criteria of $p_{\mathrm{T}} > 2$ GeV, $|\eta| < 2.8$, and $\Delta R_{\mathrm{min}}(B, \mathrm{jet}) > 0.3$, where the latter ensures that the B-hadron is located outside of any reconstructed jet. SSVs matched to a c-flavored hadron in acceptance are also categorized as true SSVs, as long as the c-flavored hadrons is separated from any B-hadron in acceptance by $\Delta R > 0.3$. The performance is evaluated on all SM processes. Events are selected in a phase space enriched with dileptonic $t\bar{t}$ events (see Sec. VI A for details).

is separated from any B-hadron in acceptance by $\Delta R > 0.3$. Events of this kind represent a minor contribution in the total calibration sample.

Figure 1(a) shows the TC-LVT efficiency to reconstruct true SSVs as a function of the generator-level ("truth") hadron p_{T}. The efficiency first increases as a function of B-hadron p_{T} as the displacement of secondary vertices also increases. The turnover at about 15 GeV is due to the fact that a B-hadron of such p_{T} is more likely to be reconstructed as a jet instead. Figure 1(b) shows the TC-LVT efficiency to reconstruct a true SSV as a function of the average number of interactions per bunch crossing (μ). While the TC-LVT efficiency is rather independent of μ, Fig. 1(c) shows that the average number of fake SSVs per event (n_f) is increasing with μ. This trend is expected from the fact that most of the fake SSVs originate from random track crossings. The fake-rate calibration is therefore carried out in two distinct μ regions.

VI. CALIBRATION OF THE SOFT SECONDARY VERTEX TAGGER

A. Measurement strategy

To account for the difference of the TC-LVT performance in data with respect to the MC simulation, correction scale factors (SFs) are estimated by performing the calibration procedure following the strategy described in this section. The calibration is carried out in a sample enriched in $t\bar{t}$ events, which overall is characterized by low to medium $E_{\mathrm{T}}^{\mathrm{miss}}$. Three SFs are extracted, as parameters of interest (POIs), with a simultaneous likelihood fit in multiple event categories (fit regions) enriched in true and fake SSVs. These are the efficiency scale factor $(\mathrm{SF}_{\mathrm{eff}})^2$ and two fake-rate scale factors $(\mathrm{SF}_{\mathrm{fake}}^{\mu_{\mathrm{L}}}, \mathrm{SF}_{\mathrm{fake}}^{\mu_{\mathrm{H}}})$.

[2]It was verified that fitting two separate efficiency scale factors from the low and high pileup data would yield compatible results.

To account for track density effects on the fake rate [Fig. 1(c)], two separate $\mathrm{SF}_{\mathrm{fake}}$ parameters are determined from low and high pileup data (μ_{L}, μ_{H}), respectively. The applicability of these correction factors to simulated events with high $E_{\mathrm{T}}^{\mathrm{miss}}$, where many SUSY searches are carried out, is validated in dedicated regions.

Events are selected based on the expected topology of the $t\bar{t}$ process, where both top quarks decay leptonically. The events are required to contain exactly two leptons (ℓ, either electrons or muons) of different flavor and opposite charge, where the leading p_{T} lepton is required to have $p_{\mathrm{T}} > 27$ GeV and the subleading lepton $p_{\mathrm{T}} > 10$ GeV. The invariant mass of the two leptons $m_{\ell\ell}$ must be > 50 GeV. Additionally, events are required to have at least one b-tagged jet with a $p_{\mathrm{T}} > 20$ GeV.

Events are further categorized based on the number of reconstructed b-jets, $\mathcal{N}_b$. Dileptonic $t\bar{t}$ events typically contain two true B-hadrons in the event, given that the branching ratio of top quarks decaying to a W boson and a b-quark is nearly 100%. Separating $t\bar{t}$ events with either exactly one or two reconstructed b-jets, for brevity referred to as $1b$ and $2b$, provide regions that are enhanced in true and fake SSVs, respectively. While $t\bar{t}$ events dominate the $2b$ region with about 96% purity, the $1b$ region has a contribution from single-top-quark processes of about 10%. However, the influence of non-$t\bar{t}$ processes in the calibration sample is negligible.

In the $1b$ region, one b-quark gives rise to a b-jet that is identified as such by the DL1r algorithm, while the second b-quark, unless missed by the b-tagging algorithm, does not give rise to a b-jet. Instead, it leads to a B-hadron that is reconstructed as a SSV. In the $2b$ region, the two b-quarks originating from the top-quark decay are already reconstructed as b-jets. The region is therefore depleted in nonreconstructed B-hadrons and most reconstructed SSVs in that region are fakes (except for events arising from $t\bar{t}+$ heavy flavor).

Events are further categorized by reconstructed SSV multiplicity, as well as into low pileup events by requiring $\mu_{\mathrm{L}} \in [0, 30)$ and high pileup events by requiring $\mu_{\mathrm{H}} \in [30, 80]$, such that each region has a similar number of events. The average μ value of the events selected in the low pileup region is 22, while the average μ value in the high pileup region is 42. Events with $\mu > 80$ represent a negligible fraction of the total number of events and are excluded from the fit regions. The region requiring two b-jets and two SSVs exhibits a yield that is too low, and is therefore excluded from the fit. Only events with $E_{\mathrm{T}}^{\mathrm{miss}} < 150$ GeV are retained for the calibration measurement regions.

For each calibration region with zero or one SSV, a validation region is defined satisfying the same event selection criteria except for the $E_{\mathrm{T}}^{\mathrm{miss}}$ requirement, which is reversed: $E_{\mathrm{T}}^{\mathrm{miss}} \geq 150$ GeV. A validation region with two SSVs is not defined since the event yield is too low. These regions validate the scale factors in an independent sample and also aim to show that the calibration results can be used in the more extreme phase space typical of many SUSY searches as well. Events with zero SSVs are used to constrain the overall $t\bar{t}$ normalization and provide a better control over systematic uncertainties associated with the modeling of the process. Among these, the $2b$ regions show the strongest constraining power due to their higher purity in $t\bar{t}$ events. Two independent normalization factors ($\mu_{t\bar{t}}$ and $\mu_{t\bar{t}}^{\text{high-}E_{\mathrm{T}}^{\mathrm{miss}}}$) are employed for the calibration regions and the high-$E_{\mathrm{T}}^{\mathrm{miss}}$ validation regions to account for an imperfect modeling of the $t\bar{t}$ process. The "0SSV $2b$, high-$E_{\mathrm{T}}^{\mathrm{miss}}$" region is the only high-$E_{\mathrm{T}}^{\mathrm{miss}}$ region used in the fit. It is inclusive in pileup and it constrains only the $\mu_{t\bar{t}}^{\text{high-}E_{\mathrm{T}}^{\mathrm{miss}}}$ parameter. Hence it provides no constraints on the calibration POIs. A summary of all the regions used in the calibration measurement is given in Table II.

In each fit region, simulated events are split according to the number of true SSVs and the number of nonreconstructed B-hadrons in acceptance, i.e. B-hadrons not matched to a SSV reconstructed by the TC-LVT, and therefore represent *missed* SSVs. Each simulated event acquires a weight composed of a tagging efficiency correction ($\mathcal{P}^{\mathrm{eff}}$), a tagging inefficiency correction ($\mathcal{P}^{\mathrm{ineff}}$) and a fake global event correction ($\mathcal{P}^{\mathrm{fake}}$). These corrections are a function of the number of true and missed SSVs, $\mathcal{N}_{\mathrm{true}}$ and $\mathcal{N}_{\mathrm{miss}}$, respectively, the efficiency in simulation, $\varepsilon_{\mathrm{SSV}}$, the expected number of fake SSVs per event from simulation n_f, and the SF POIs as stated in Eq. (1):

$$
\begin{aligned}
&w(\mathcal{N}_{\mathrm{true}}, \mathcal{N}_{\mathrm{miss}}, \mathcal{N}_{\mathrm{SSV}}) \\
&= \mathcal{P}^{\mathrm{eff}} \times \mathcal{P}^{\mathrm{ineff}} \times \mathcal{P}^{\mathrm{fake}} \\
&= \prod_{1}^{\mathcal{N}_{\mathrm{true}}} \mathrm{SF}_{\mathrm{eff}} \times \prod_{1}^{\mathcal{N}_{\mathrm{miss}}} \frac{1 - \mathrm{SF}_{\mathrm{eff}} \cdot \varepsilon_{\mathrm{ssv}}(\mathcal{N}_b)}{1 - \varepsilon_{\mathrm{ssv}}(\mathcal{N}_b)} \\
&\quad \times \prod_{\mu=\mu_{\mathrm{L}},\mu_{\mathrm{H}}} \frac{\mathrm{Poiss}(\mathcal{N}_{\mathrm{ssv}} - \mathcal{N}_{\mathrm{true}} | \mathrm{SF}_{\mathrm{fake}}(\mu) \cdot n_f(\mu, \mathcal{N}_b))}{\mathrm{Poiss}(\mathcal{N}_{\mathrm{ssv}} - \mathcal{N}_{\mathrm{true}} | n_f(\mu, \mathcal{N}_b))}. \quad (1)
\end{aligned}
$$

The SF POIs are common for the $1b$ and $2b$ selections and inclusive in B-hadron p_{T}. The last term of the equation describes the SF correction to the fake rate as a ratio of conditional Poisson probabilities. This is calculated, globally per event, as the conditional Poisson probability of observing the number of fake reconstructed SSVs in the event ($\mathcal{N}_{\mathrm{ssv}} - \mathcal{N}_{\mathrm{true}}$) given the average number of fake SSVs predicted by the simulation [$n_f(\mu, \mathcal{N}_b)$], where $\mathcal{N}_b$ is the number of reconstructed b-jets. In the numerator of this term, n_f is corrected by $\mathrm{SF}_{\mathrm{fake}}$, which is one of the free parameters of interest in the fit. Products over $\mathcal{N}_{\mathrm{true}}$ and $\mathcal{N}_{\mathrm{miss}}$ are truncated at four, i.e. consider only events with up to four B-hadrons in acceptance.

TABLE II. Summary of all the selections used for the calibration measurement and its validation. The requirement on SSV multiplicity ($\mathcal{N}_{\mathrm{SSV}}$), b-jet multiplicity ($\mathcal{N}_b$), average number of interactions per bunch crossing (μ), and $E_{\mathrm{T}}^{\mathrm{miss}}$ are indicated in the table. The last column indicates which parameters of the fit are constrained or validated by each selection.

Region label	$\mathcal{N}_{\mathrm{SSV}}$	$\mathcal{N}_b$	μ	$E_{\mathrm{T}}^{\mathrm{miss}}$	Purpose
0SSV $2b$, μ_{L}	0	2	[0, 30)	<150	Constrain $\mu_{t\bar{t}}$
0SSV $2b$, μ_{H}	0	2	[30, 80]	<150	Constrain $\mu_{t\bar{t}}$
0SSV $2b$, high-$E_{\mathrm{T}}^{\mathrm{miss}}$	0	2	⋯	≥150	Constrain $\mu_{t\bar{t}}^{\text{high-}E_{\mathrm{T}}^{\mathrm{miss}}}$
1SSV $1b$, μ_{L}	1	1	[0, 30)	<150	Constrain $\mathrm{SF}_{\mathrm{eff}}$, $\mathrm{SF}_{\mathrm{fake}}^{\mu_{\mathrm{L}}}$
1SSV $1b$, μ_{H}	1	1	[30, 80]	<150	Constrain $\mathrm{SF}_{\mathrm{eff}}$, $\mathrm{SF}_{\mathrm{fake}}^{\mu_{\mathrm{H}}}$
1SSV $1b$, μ_{L}, high-$E_{\mathrm{T}}^{\mathrm{miss}}$	1	1	[0, 30)	≥150	Validate $\mathrm{SF}_{\mathrm{eff}}$, $\mathrm{SF}_{\mathrm{fake}}^{\mu_{\mathrm{L}}}$
1SSV $1b$, μ_{H}, high-$E_{\mathrm{T}}^{\mathrm{miss}}$	1	1	[30, 80]	≥150	Validate $\mathrm{SF}_{\mathrm{eff}}$, $\mathrm{SF}_{\mathrm{fake}}^{\mu_{\mathrm{H}}}$
1SSV $2b$, μ_{L}	1	2	[0, 30)	<150	Constrain $\mathrm{SF}_{\mathrm{eff}}$, $\mathrm{SF}_{\mathrm{fake}}^{\mu_{\mathrm{L}}}$
1SSV $2b$, μ_{H}	1	2	[30, 80]	<150	Constrain $\mathrm{SF}_{\mathrm{eff}}$, $\mathrm{SF}_{\mathrm{fake}}^{\mu_{\mathrm{H}}}$
1SSV $2b$, μ_{L}, high-$E_{\mathrm{T}}^{\mathrm{miss}}$	1	2	[0, 30)	≥150	Validate $\mathrm{SF}_{\mathrm{eff}}$, $\mathrm{SF}_{\mathrm{fake}}^{\mu_{\mathrm{L}}}$
1SSV $2b$, μ_{H}, high-$E_{\mathrm{T}}^{\mathrm{miss}}$	1	2	[30, 80]	≥150	Validate $\mathrm{SF}_{\mathrm{eff}}$, $\mathrm{SF}_{\mathrm{fake}}^{\mu_{\mathrm{H}}}$
2SSV $1b$, μ_{L}	2	1	[0, 30)	<150	Constrain $\mathrm{SF}_{\mathrm{eff}}$, $\mathrm{SF}_{\mathrm{fake}}^{\mu_{\mathrm{L}}}$
2SSV $1b$, μ_{H}	2	1	[30, 80]	<150	Constrain $\mathrm{SF}_{\mathrm{eff}}$, $\mathrm{SF}_{\mathrm{fake}}^{\mu_{\mathrm{H}}}$

Events with higher B-hadron multiplicities are negligible. The parameters $\varepsilon_{\mathrm{SSV}}$ and n_f are estimated in simulated $t\bar{t}$ events as a function of $\mathcal{N}_b$ (and in two bins of μ for n_f) and provided as an input to the weight calculation. The values used are shown in Table III. The performance difference between the $1b$ and the $2b$ selections is due to differences between the SSV momentum distribution in the two regions. These parameters were also estimated by using Herwig as alternative parton shower modeling generator. It was found that n_f does not depend on the shower generator choice. The efficiency, $\varepsilon_{\mathrm{SSV}}$, is also very similar between the two parton shower generators for B-hadron p_{T} smaller than 10 GeV, while it is about 15% smaller for the alternative shower simulation for larger B-hadron p_{T}. This difference is also considered in the systematic uncertainties of the measurement (Sec. VI B).

B. Systematic uncertainties

Various sources of uncertainties related to the underlying theoretical models for simulated processes as well as detector effects are considered in the measurement of the scale factors and summarized in this section. The systematic uncertainties are introduced to the likelihood function in the form of Gaussian-constrained nuisance parameters θ_i and fitted simultaneously with the POIs, as introduced in the previous section.

TABLE III. Input values to weight calculation of Eq. (1) obtained from simulated events. Relative statistical uncertainties amount to less than 1% in all cases.

Parameter	$\mathcal{N}_b = 1$	$\mathcal{N}_b = 2$
$\varepsilon_{\mathrm{ssv}}$	0.0173	0.0116
$n_f(\mu_{\mathrm{L}})$	0.0105	0.0078
$n_f(\mu_{\mathrm{H}})$	0.0149	0.0125

Systematic uncertainties related to the track selection efficiency are determined through dedicated simulated samples where the amount of tracker material and the physical models were altered in the Geant4 implementation of the detector. Residual alignment uncertainties between data and simulation on the track parameters, including the transverse (d_0) and longitudinal (z_0) impact parameters and the track sagitta, as well as uncertainties on the impact parameter resolution are considered. These effects, along with systematic variations of the number of fake tracks, are applied to the tracks used in the TC-LVT reconstruction algorithm, which is reexecuted for each source of uncertainty such that the number of true and fake SSVs in each event is reevaluated.

A variation in the pileup reweighting of simulated events is included to cover the uncertainty on the ratio of the predicted inelastic cross section in simulations compared to the one measured in data.

Uncertainties related to the energy scale (JES) and resolution [66] of hadronic jets are derived by combining information from test-beam data, LHC collision data, and simulation. Uncertainties related to the jet energy resolution have a negligible impact on the measurement. Among the sources of uncertainty contributing to the JES, the most important uncertainties for these measurements are those related to the modeling of the pileup, flavor composition of the jet calibration sample, and the different response for each jet flavor (see Ref. [66] for details). In addition, uncertainties related to the differences between data and simulation of the performance of the JVT algorithm [67] are accounted for.

Dedicated measurements are carried out to assess the performance of the DL1r b-tagging algorithm on b-jets [2]

and the mistagging performance for c-jets [71] and light-jets [72]. These measurements derive corrections from data control samples, which are applied to account for differences between data and simulation in the efficiency and mistag rate of the b-tagging algorithm. The corrections used in this analysis are derived in pseudocontinuous bins of the tagger discriminant distribution [2]. A large number of uncertainties are considered. A principal component analysis is performed on these uncertainties, and the resulting uncertainties are taken as uncorrelated components for the measurement described here. An uncertainty in the relative fraction of quark versus gluon jets of 50% is also applied to all simulated samples.

The combined 2015–2018 integrated luminosity, which is obtained using the LUCID-2 detector for the primary measurement and complemented by measurements using the inner detector and calorimeters, has an uncertainty of 0.83% [21].

The reconstruction, identification, and isolation efficiencies of electrons and muons, as well as the efficiency of the trigger used to record the events, differ slightly between data and simulation. These differences are compensated for by dedicated SFs, which are measured using tag-and-probe techniques on $Z \to \ell^+\ell^-$ experimental and simulated samples [59,62]. The SFs, with uncertainties, are applied as corrections to the simulated event weights. Additional sources of uncertainty arise from the corrections used to adjust the lepton momentum scale and resolution, which are also propagated to the simulated samples. All lepton-related uncertainties have an impact on the measurement smaller than 0.5%.

Uncertainties related to the modeling of the $t\bar{t}$ process include effects associated with missing higher-order corrections in the perturbative expansion of the partonic cross section and the PDF uncertainties. The first point is addressed by varying the renormalization (μ_r) and factorization (μ_f) scales, while the latter is evaluated following the PDF4LHC recommendations [73]. The α_s uncertainty is derived using the same PDF set but with two different α_s values. The uncertainties from the PDF and α_s variations are added in quadrature.

For the uncertainties due to parton shower and hadronization and due to the NLO matching, the nominal POWHEG BOX + Pythia8 $t\bar{t}(5\mathrm{FS})$ sample is compared with the POWHEG BOX + Herwig7 $t\bar{t}(5\mathrm{FS})$ sample. To evaluate the effect of the amount of ISR and FSR on the measurement, the settings of the nominal POWHEG BOX + Pythia8 $t\bar{t}(5\mathrm{FS})$ sample are varied. The uncertainty due to ISR is estimated by simultaneously changing μ_r and μ_f in the ME and $\mu_{\mathrm{R}}^{\mathrm{ISR}}$ in the PS, while the uncertainty due to FSR is estimated by changing $\mu_{\mathrm{R}}^{\mathrm{FSR}}$ in the PS.

TABLE IV. Postfit yields, including systematic uncertainties, in all calibration regions. Due to correlations, systematic uncertainties on the individual samples do not necessarily add up in quadrature to the total uncertainty. $t\bar{t}$ events are assigned to the "$t\bar{t}$ fakes" category if the event contains at least one fake SSV.

	0SSV 2b, μ_L	0SSV 2b, μ_H	1SSV 1b, μ_L	2SSV 1b, μ_L	1SSV 2b, μ_L	1SSV 1b, μ_H	2SSV 1b, μ_H	1SSV 2b, μ_H
$t\bar{t}$ true	194940 ± 20150	225310 ± 21660	5760 ± 610	62 ± 10	1316 ± 164	6530 ± 640	63 ± 11	1447 ± 177
$t\bar{t}$ fakes	⋯	⋯	2350 ± 387	177 ± 32	2348 ± 323	3697 ± 485	277 ± 38	4012 ± 423
Single top	6814 ± 840	8161 ± 1006	781 ± 100	22 ± 5	132 ± 18	1102 ± 140	36 ± 7	207 ± 29
Others	960 ± 190	1130 ± 230	180 ± 40	5 ± 1	30 ± 6	270 ± 60	7 ± 2	40 ± 8
Total predicted	202400 ± 900	234700 ± 900	9060 ± 100	266 ± 12	3830 ± 60	11600 ± 110	384 ± 17	5690 ± 70
Data	202359	234733	9068	279	3806	11589	381	5703

TABLE V. Postfit yields, including systematic uncertainties, in all high-$E_{\mathrm{T}}^{\mathrm{miss}}$ validation regions. The "0SSV 2b" region is used to constrain the $t\bar{t}$ normalization in all validation regions. Due to correlations, systematic uncertainties on the individual samples do not necessarily add up in quadrature to the total uncertainty. $t\bar{t}$ events are assigned to the "$t\bar{t}$ fakes" category if the event contains at least one fake SSV.

	0SSV 2b high-$E_{\mathrm{T}}^{\mathrm{miss}}$	1SSV 2b, μ_L high-$E_{\mathrm{T}}^{\mathrm{miss}}$	1SSV 2b, μ_H high-$E_{\mathrm{T}}^{\mathrm{miss}}$	1SSV 1b, μ_L high-$E_{\mathrm{T}}^{\mathrm{miss}}$	1SSV 1b, μ_H high-$E_{\mathrm{T}}^{\mathrm{miss}}$
$t\bar{t}$ true	23730 ± 3010	112 ± 29	133 ± 36	471 ± 108	569 ± 125
$t\bar{t}$ fakes	⋯	141 ± 34	263 ± 55	164 ± 37	282 ± 57
Single top	1618 ± 182	14 ± 3	27 ± 6	49 ± 9	73 ± 12
Others	270 ± 50	4 ± 1	7 ± 1	10 ± 2	14 ± 3
Total predicted	25600 ± 160	270 ± 40	430 ± 60	690 ± 110	940 ± 140
Data	25601	245	418	678	808

Certain regions in the calibration measurement contain a sizable contribution of up to 13% of $t\bar{t}$ events with additional heavy-flavor quarks. Various measurements of this process have shown that the simulation consistently underestimates the contribution [74], therefore an additional one-sided uncertainty of 28% is introduced to account for this discrepancy.

Single-top-quark processes contribute subdominantly in some parts of the phase space and are governed by an additional uncertainty stemming from different ways to treat the interference between $t\bar{t}$ and tW production. The nominal tW samples use the diagram removal scheme, while the alternative samples use the diagram subtraction scheme [44,45].

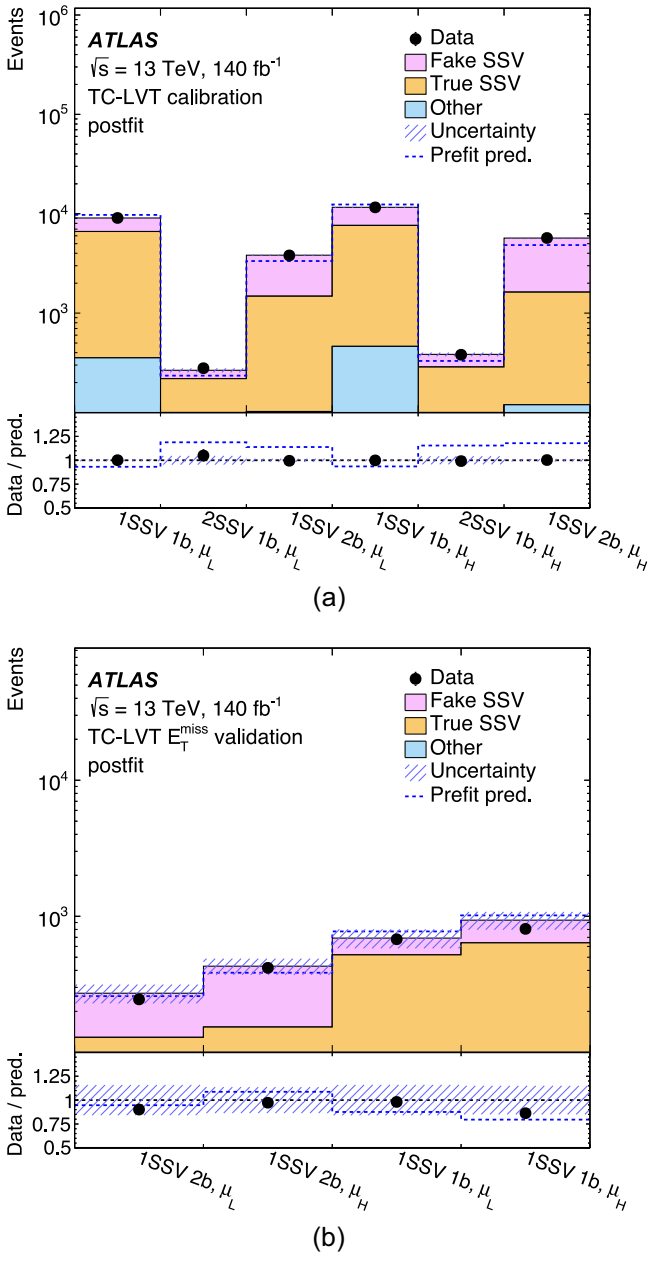

FIG. 2. Summary of the fit results in (a) calibration regions and (b) validation regions. The prediction is separated into top-quark events (i.e. $t\bar{t}$ and single-top-quark processes) containing only true SSVs (true) and events containing at least one fake SSV (fakes). The "Other" category contains contributions from non-top-quark processes. The bottom panel shows the ratio of the data and the prefit (dashed lines) and postfit (points) prediction. The hashed band shows the full uncertainty of the prediction.

C. Calibration results

The nine calibration regions described in Sec. VI A are included in a simultaneous maximum-likelihood fit using five unconstrained parameters (two $t\bar{t}$ normalization parameters and the three POIs: $\mathrm{SF}_{\mathrm{eff}}$, $\mathrm{SF}_{\mathrm{fake}}^{\mu_{\mathrm{L}}}$, $\mathrm{SF}_{\mathrm{fake}}^{\mu_{\mathrm{H}}}$). Systematic uncertainties, as described in Sec. VI B, are treated in the fit as $\mathcal{O}(100)$ nuisance parameters with Gaussian prior. The width of the Gaussian, σ, is equal to the systematic uncertainty corresponding to the nuisance parameter. Uncertainties are inclusive in B-hadron p_{T}. All common sources of uncertainties are treated as correlated across eight of the nine measurement regions but uncorrelated with respect to the "0SSV 2b, high-$E_{\mathrm{T}}^{\mathrm{miss}}$" region used to constrain the $\mu_{t\bar{t}}^{\text{high-}E_{\mathrm{T}}^{\mathrm{miss}}}$ normalization parameter. This treatment guarantees that no constraint is imposed on the POIs from the high-$E_{\mathrm{T}}^{\mathrm{miss}}$ normalization region. The pileup uncertainties are the only exception to this treatment. These uncertainties are also treated as uncorrelated between regions with zero or at least one SSV and they are also uncorrelated between high- and low-μ regions.

After the fit, a good agreement between the observed data and the prediction is obtained. Postfit yields and their uncertainties are summarized for the calibration regions in Table IV, the validation regions in Table V, and shown in Fig. 2. Both calibration regions and high-$E_{\mathrm{T}}^{\mathrm{miss}}$ validation regions are included in the latter. The POIs of the fit, summarized in Table VI, are extracted in the calibration regions and applied in the validation regions, which also show good postfit agreement between the data and the prediction.

Selected postfit distributions of the SSV transverse momentum are shown in Fig. 3 for a subset of the calibration and validation regions. This calibration targets

TABLE VI. Fit results, with uncertainties, for the five unconstrained parameters.

Fitted parameter	Value
$\mathrm{SF}_{\mathrm{eff}}$	0.86 ± 0.10
$\mathrm{SF}_{\mathrm{fake}}^{\mu_{\mathrm{L}}}$	1.63 ± 0.15
$\mathrm{SF}_{\mathrm{fake}}^{\mu_{\mathrm{H}}}$	1.58 ± 0.13
$\mu_{t\bar{t}}$	0.96 ± 0.14
$\mu_{t\bar{t}}^{\text{high-}E_{\mathrm{T}}^{\mathrm{miss}}}$	0.91 ± 0.19

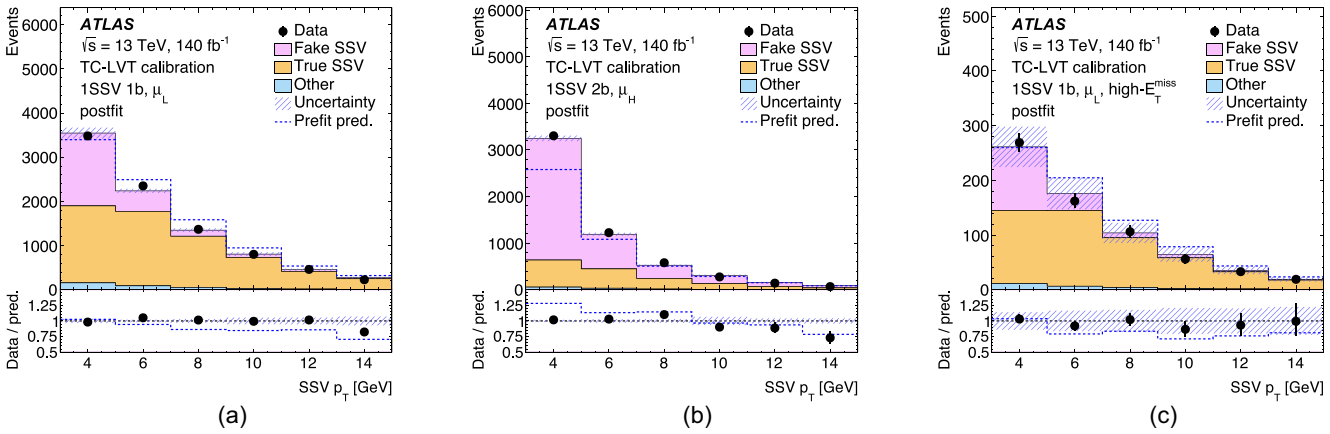

FIG. 3. Distribution of the SSV p_{T} in (a),(b) two calibration regions and (c) one validation region. The prediction, which is shown postfit, is separated into top-quark events (i.e. $t\bar{t}$ and single-top-quark processes) containing only true SSVs (true) and events containing at least one fake SSV (fakes). The "Other" category contains contributions from non-top-quark processes. Hashed bands indicate the full uncertainty of the prediction. The last bin contains also the events in the overflow.

events with SSV transverse momentum smaller than 20 GeV. Only a very small fraction of events considered in the calibration contain an SSV with a transverse momentum above 15 GeV. The overall good agreement between the observed data and the prediction as a function of p_{T} indicates that the assumption of p_{T}-independent SFs holds and supports the applicability of this calibration to analyses characterized by SSV p_{T} spectra significantly different from that in the calibration sample. The small discrepancy between the experimental data and the simulation in the SSV p_{T} bin 13–15 GeV, indicates a possible p_{T} dependence of the calibration for values of SSV p_{T}

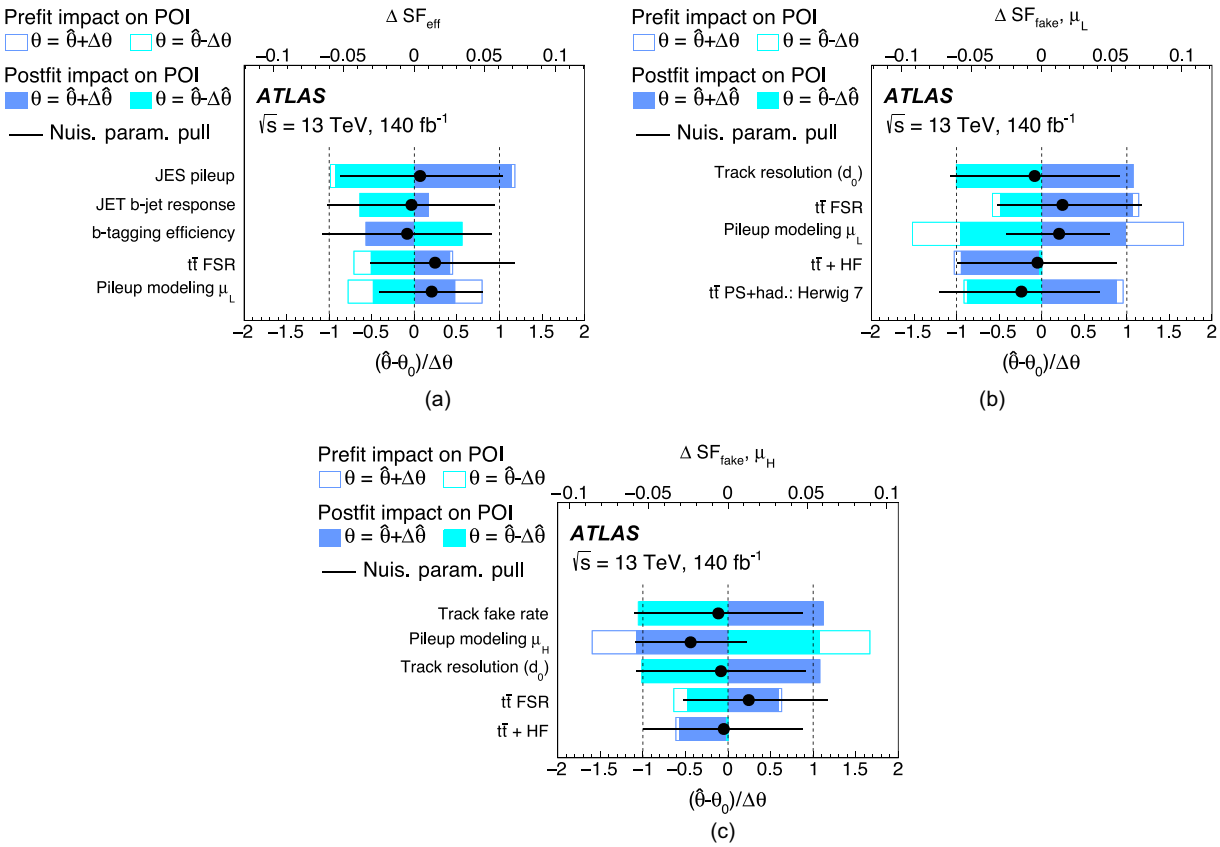

FIG. 4. The five nuisance parameters with the largest impact on the three calibration scale factors (a) $\mathrm{SF}_{\mathrm{eff}}$, (b) $\mathrm{SF}_{\mathrm{fake}}^{\mu_{\mathrm{L}}}$, and (c) $\mathrm{SF}_{\mathrm{fake}}^{\mu_{\mathrm{H}}}$.

beyond 15 GeV, which are provided as the validity limit for the applicability of this calibration. Further investigations would be needed in order to extend the calibration beyond this SSV p_{T} range.

The efficiency scale factor is found to be smaller than one by about 15%, while the two fake rate scale factors are found to be greater than one by about 60% (Table VI). The underlying causes of these effects are currently not fully understood, albeit these results are qualitatively consistent with those measured for b-tagging in jets. The fitted values for the $t\bar{t}$ normalization are consistent with factors obtained in previous measurements by the ATLAS Collaboration [75] targeting a similar phase space. The nuisance parameters are only mildly constrained, with the exception of the parameters associated with the modeling of pileup. The fit constrains the pileup uncertainties to about 50% of its original value. This is expected because the pileup uncertainties aim to cover the residual differences of data and simulation over an inclusive phase space, whereas the analysis bins are split into two separate μ regimes.

The impact of the five leading systematic uncertainties on the three POIs are presented in Fig. 4. A summary of the impact of all leading systematic uncertainties, grouped by uncertainty sources, is given in Table VII. Impacts are calculated by estimating, for each nuisance parameter, the difference between the fitted POI in the nominal maximum-likelihood fit and a second fit performed by fixing the nuisance parameter to its nominal maximum-likelihood estimator plus one σ of its Gaussian prior ($\hat{\theta} + 1\sigma$). Uncertainties related to the pileup modeling and the modeling of extra-jet radiation in the $t\bar{t}$ background are among the dominant sources of systematic uncertainties for all SFs. Additionally, the uncertainties related to b-jet identification, jet energy scale, and jet flavor composition are important for $\mathrm{SF}_{\mathrm{eff}}$, while track-related uncertainties dominate for $\mathrm{SF}_{\mathrm{fake}}^{\mu_{\mathrm{L}}}$ and $\mathrm{SF}_{\mathrm{fake}}^{\mu_{\mathrm{H}}}$. Statistical uncertainties are below 1% in this measurement.

TABLE VII. Summary of the impact of the dominant systematic uncertainties in this calibration for the three calibration scale factors. All systematic uncertainties are fully correlated bin by bin, except special cases as explained in the text. In the case of correlated systematic uncertainties, the relative sign of the uncertainty for each measurement is taken into account, even if not shown here.

Uncertainty impact	$\mathrm{SF}_{\mathrm{eff}}$ (%)	$\mathrm{SF}_{\mathrm{fake}}^{\mu_{\mathrm{L}}}$ (%)	$\mathrm{SF}_{\mathrm{fake}}^{\mu_{\mathrm{H}}}$ (%)
Jet energy scale	7	3	2
Flavor tagging	3	3	2.5
$t\bar{t}$ modeling	3	6	3
$t\bar{t}$ heavy-flavor modeling	1.5	6	3
Pileup	3	6	6
Track resolution	<1	6.5	6
Track fake rate	<1	<1	6

VII. CONCLUSION

The reconstruction and identification of jets that originate from the hadronization process of b-quarks is an important component in measurements and searches carried out by the ATLAS experiment. Various tagging algorithms and techniques are in place, covering a large b-jet p_{T} range. A dedicated calibration of the TC-LVT algorithm, which focuses on the identification of B-hadrons with such low p_{T} that they do not give rise to a reconstructed jet ($p_{\mathrm{T}} < 20$ GeV), is presented for the first time in this paper. The result of the calibration measurement is a set of scale factors that can be used to correct the performance of the TC-LVT algorithm in simulation to match that observed in data. These results improve and extend the previous calibration of this algorithm obtained in the context of bottom squark searches in the compressed mass regime.

The measurement is carried out using 140 fb^{-1} of data from pp collisions collected with the ATLAS detector during LHC Run 2 at a center-of-mass energy of 13 TeV. A data sample containing predominantly dileptonic $t\bar{t}$ events is selected, by requiring exactly one muon and one electron of opposite electric charge. Various orthogonal regions are defined to facilitate the simultaneous measurement of efficiency and fake-rate scale factors. Simulated events are categorized based on the presence of true or fake SSVs, i.e. SSVs matched to a real B-hadron and SSVs mainly arising from random track crossings involving tracks from additional proton-proton interactions occurring in the same bunch crossing, reconstructed by the TC-LVT algorithm.

By separating events into regions with different b-jet multiplicities, different numbers of SSVs, and low and high pileup, the different contributions of true and fake SSVs in these regions can be exploited in a combined likelihood fit to extract the scale factors. Auxiliary measurements are included as well, to reduce the dependence on any potential mismodeling of the $t\bar{t}$ process in the high missing transverse momentum regime. Systematic uncertainties are included as nuisance parameters in the fit.

A single efficiency scale factor, $\mathrm{SF}_{\mathrm{eff}} = 0.86 \pm 0.10$, is determined. Two pileup-dependent mistag rate scale factors, $\mathrm{SF}_{\mathrm{fake}}^{\mu_{\mathrm{L}}} = 1.63 \pm 0.15$ and $\mathrm{SF}_{\mathrm{fake}}^{\mu_{\mathrm{H}}} = 1.58 \pm 0.13$, are measured. These scale factors are valid for SSV transverse momenta between 3 and 15 GeV. The resulting efficiency in data for the TC-LVT algorithm ranges from 1% to 12% in the p_{T} range 3–15 GeV. The TC-LVT algorithm and calibration described in this paper can significantly improve the sensitivity in various beyond-the-SM searches as they provide a novel and effective tool to reconstruct and identify events that contain low-momentum b-quarks.

ACKNOWLEDGMENTS

We thank CERN for the very successful operation of the LHC and its injectors, as well as the support staff at CERN

and at our institutions worldwide without whom ATLAS could not be operated efficiently. The crucial computing support from all WLCG partners is acknowledged gratefully, in particular from CERN, the ATLAS Tier-1 facilities at TRIUMF/SFU (Canada), NDGF (Denmark, Norway, Sweden), CC-IN2P3 (France), KIT/GridKA (Germany), INFN-CNAF (Italy), NL-T1 (Netherlands), PIC (Spain), RAL (UK), and BNL (USA), the Tier-2 facilities worldwide and large non-WLCG resource providers. Major contributors of computing resources are listed in Ref. [76]. We gratefully acknowledge the support of ANPCyT, Argentina; YerPhI, Armenia; ARC, Australia; BMWFW and FWF, Austria; ANAS, Azerbaijan; CNPq and FAPESP, Brazil; NSERC, NRC, and CFI, Canada; CERN; ANID, Chile; CAS, MOST, and NSFC, China; Minciencias, Colombia; MEYS CR, Czech Republic; DNRF and DNSRC, Denmark; IN2P3-CNRS and CEA-DRF/IRFU, France; SRNSFG, Georgia; BMBF, HGF, and MPG, Germany; GSRI, Greece; RGC and Hong Kong SAR, China; ISF and Benoziyo Center, Israel; INFN, Italy; MEXT and JSPS, Japan; CNRST, Morocco; NWO, Netherlands; RCN, Norway; MNiSW, Poland; FCT, Portugal; MNE/IFA, Romania; MESTD, Serbia; MSSR, Slovakia; ARRS and MIZŠ, Slovenia; DSI/NRF, South Africa; MICINN, Spain; SRC and Wallenberg Foundation, Sweden; SERI, SNSF, and Cantons of Bern and Geneva, Switzerland; MOST, Taipei; TENMAK, Türkiye; STFC, United Kingdom; DOE and NSF, U.S. Individual groups and members have received support from BCKDF, CANARIE, CRC, and DRAC, Canada; CERN-CZ, FORTE, and PRIMUS, Czech Republic; COST, ERC, ERDF, Horizon 2020, ICSC-NextGenerationEU, and Marie Skłodowska-Curie Actions, European Union; Investissements d'Avenir Labex, Investissements d'Avenir Idex, and ANR, France; DFG and AvH Foundation, Germany; Herakleitos, Thales, and Aristeia programmes cofinanced by EU-ESF and the Greek NSRF, Greece; BSF-NSF and MINERVA, Israel; Norwegian Financial Mechanism 2014-2021, Norway; NCN and NAWA, Poland; La Caixa Banking Foundation, CERCA Programme Generalitat de Catalunya, and PROMETEO and GenT Programmes Generalitat Valenciana, Spain; Göran Gustafssons Stiftelse, Sweden; and The Royal Society and Leverhulme Trust, United Kingdom. In addition, individual members wish to acknowledge support from CERN: European Organization for Nuclear Research (CERN PJAS); Chile: Agencia Nacional de Investigación y Desarrollo (FONDECYT 1190886, FONDECYT 1230812, FONDECYT 1230987); China: Chinese Ministry of Science and Technology (MOST-2023YFA1605700), National Natural Science Foundation of China (NSFC-12175119, NSFC-12275265, NSFC-12075060); Czech Republic: Czech Science Foundation (GACR—24-11373S), Ministry of Education Youth and Sports (FORTE CZ.02.01.01/00/22_008/0004632), PRIMUS Research Programme (PRIMUS/21/SCI/017); EU: H2020 European Research Council (ERC-101002463); European Union: European Research Council (ERC-948254, ERC-101089007), Horizon 2020 Framework Programme (MUCCA—CHIST-ERA-19-XAI-00), European Union, Future Artificial Intelligence Research (FAIR-NextGenerationEU PE00000013), Italian Center for High Performance Computing, Big Data and Quantum Computing (ICSC, NextGenerationEU); France: Agence Nationale de la Recherche (ANR-20-CE31-0013, ANR-21-CE31-0013, ANR-21-CE31-0022), Investissements d'Avenir Labex (ANR-11-LABX-0012); Germany: Baden-Württemberg Stiftung (BW Stiftung-Postdoc Eliteprogramme), Deutsche Forschungsgemeinschaft (DFG-469666862, DFG-CR 312/5-2); Italy: Istituto Nazionale di Fisica Nucleare (ICSC, NextGenerationEU); Japan: Japan Society for the Promotion of Science (JSPS KAKENHI JP21H05085, JSPS KAKENHI JP22H01227, JSPS KAKENHI JP22H04944, JSPS KAKENHI JP22KK0227); Netherlands: Netherlands Organisation for Scientific Research (NWO Veni 2020—VI.Veni.202.179); Norway: Research Council of Norway (RCN-314472); Poland: Polish National Agency for Academic Exchange (PPN/PPO/2020/1/00002/U/00001), Polish National Science Centre (NCN 2021/42/E/ST2/00350, NCN OPUS nr 2022/47/B/ST2/03059, NCN UMO-2019/34/E/ST2/00393, UMO-2020/37/B/ST2/01043, UMO-2021/40/C/ST2/00187, UMO-2022/47/O/ST2/00148, UMO-2023/49/B/ST2/04085); Slovenia: Slovenian Research Agency (ARIS Grant No. J1-3010); Spain: Generalitat Valenciana (Artemisa, FEDER, IDIFEDER/2018/048), Ministry of Science and Innovation (MCIN and NextGenEU PCI2022-135018-2, MICIN and FEDER PID2021-125273NB, RYC2019-028510-I, RYC2020-030254-I, RYC2021-031273-I, RYC2022-038164-I), PROMETEO and GenT Programmes Generalitat Valenciana (CIDEGENT/2019/023, CIDEGENT/2019/027); Sweden: Swedish Research Council (Swedish Research Council 2023-04654, VR 2018-00482, VR 2022-03845, VR 2022-04683, VR 2023-03403, VR Grant No. 2021-03651), Knut and Alice Wallenberg Foundation (KAW 2018.0157, KAW 2018.0458, KAW 2019.0447, KAW 2022.0358); Switzerland: Swiss National Science Foundation (SNSF—PCEFP2_194658); United Kingdom: Leverhulme Trust (Leverhulme Trust RPG-2020-004), Royal Society (NIF-R1-231091); U.S.: U.S. Department of Energy (ECA DE-AC02-76SF00515), Neubauer Family Foundation.

[1] ATLAS Collaboration, Performance of b-jet identification in the ATLAS experiment, J. Instrum. **11**, P04008 (2016).

[2] ATLAS Collaboration, ATLAS b-jet identification performance and efficiency measurement with $t\bar{t}$ events in pp collisions at $\sqrt{s} = 13$ TeV, Eur. Phys. J. C **79**, 970 (2019).

[3] ATLAS Collaboration, ATLAS flavour-tagging algorithms for the LHC Run 2 pp collision dataset, Eur. Phys. J. C **83**, 681 (2023).

[4] Y. Golfand and E. Likhtman, Extension of the algebra of Poincaré group generators and violation of P invariance, Pis'ma Zh. Eksp. Teor. Fiz. **13**, 452 (1971) [JETP Lett. **13**, 323 (1971)].

[5] D. Volkov and V. Akulov, Is the neutrino a Goldstone particle?, Phys. Lett. **46B**, 109 (1973).

[6] J. Wess and B. Zumino, Supergauge transformations in four dimensions, Nucl. Phys. **B70**, 39 (1974).

[7] J. Wess and B. Zumino, Supergauge invariant extension of quantum electrodynamics, Nucl. Phys. **B78**, 1 (1974).

[8] S. Ferrara and B. Zumino, Supergauge invariant Yang-Mills theories, Nucl. Phys. **B79**, 413 (1974).

[9] A. Salam and J. Strathdee, Super-symmetry and non-Abelian gauges, Phys. Lett. **51B**, 353 (1974).

[10] ATLAS Collaboration, Search for Higgs boson decays into two new low-mass spin-0 particles in the $4b$ channel with the ATLAS detector using pp collisions at $\sqrt{s} = 13$ TeV, Phys. Rev. D **102**, 112006 (2020).

[11] T. Robens, T. Stefaniak, and J. Wittbrodt, Two-real-scalar-singlet extension of the SM: LHC phenomenology and benchmark scenarios, Eur. Phys. J. C **80** (2020).

[12] ATLAS Collaboration, Search for new phenomena in final states with b-jets and missing transverse momentum in $\sqrt{s} = 13$ TeV pp collisions with the ATLAS detector, J. High Energy Phys. 05 (**2021**) 093.

[13] ATLAS Collaboration, Search for new phenomena with top quark pairs in final states with one lepton, jets, and missing transverse momentum in pp collisions at $\sqrt{s} = 13$ TeV with the ATLAS detector, J. High Energy Phys. 04 (2021) 174.

[14] CMS Collaboration, Search for direct production of supersymmetric partners of the top quark in the all-jets final state in proton-proton collisions at $\sqrt{s} = 13$ TeV, J. High Energy Phys. 10 (2017) 005.

[15] ATLAS Collaboration, The ATLAS Experiment at the CERN Large Hadron Collider, J. Instrum. **3**, S08003 (2008).

[16] ATLAS Collaboration, ATLAS insertable B-Layer: Technical design report, Reports No. ATLAS-TDR-19 and No. CERN-LHCC-2010-013, 2010, https://cds.cern.ch/record/1291633; Addendum: Reports No. ATLAS-TDR-19-ADD-1 and No. CERN-LHCC-2012-009, 2012, https://cds.cern.ch/record/1451888.

[17] B. Abbott *et al.*, Production and integration of the ATLAS insertable B-layer, J. Instrum. **13**, T05008 (2018).

[18] G. Avoni *et al.*, The new LUCID-2 detector for luminosity measurement and monitoring in ATLAS, J. Instrum. **13**, P07017 (2018).

[19] ATLAS Collaboration, Performance of the ATLAS trigger system in 2015, Eur. Phys. J. C **77**, 317 (2017).

[20] ATLAS Collaboration, Software and computing for Run 3 of the ATLAS experiment at the LHC, arXiv:2404.06335.

[21] ATLAS Collaboration, Luminosity determination in pp collisions at $\sqrt{s} = 13$ TeV using the ATLAS detector at the LHC, Eur. Phys. J. C **83**, 982 (2023).

[22] ATLAS Collaboration, Performance of electron and photon triggers in ATLAS during LHC Run 2, Eur. Phys. J. C **80**, 47 (2020).

[23] ATLAS Collaboration, Performance of the ATLAS muon triggers in Run 2, J. Instrum. **15**, P09015 (2020).

[24] ATLAS Collaboration, ATLAS data quality operations and performance for 2015–2018 data-taking, J. Instrum. **15**, P04003 (2020).

[25] ATLAS Collaboration, The ATLAS simulation infrastructure, Eur. Phys. J. C **70**, 823 (2010).

[26] S. Agostinelli *et al.*, Geant4—A simulation toolkit, Nucl. Instrum. Methods Phys. Res., Sect. A **506**, 250 (2003).

[27] T. Sjöstrand, S. Mrenna, and P. Skands, A brief introduction to Pythia 8.1, Comput. Phys. Commun. **178**, 852 (2008).

[28] R. D. Ball *et al.* (NNPDF Collaboration), Parton distributions with LHC data, Nucl. Phys. **B867**, 244 (2013).

[29] ATLAS Collaboration, The Pythia8 A3 tune description of ATLAS minimum bias and inelastic measurements incorporating the Donnachie–Landshoff diffractive model, Report No. ATL-PHYS-PUB-2016-017, 2016, https://cds.cern.ch/record/2206965.

[30] ATLAS Collaboration, Measurement of the inelastic proton-proton cross section at $\sqrt{s} = 13$ TeV with the ATLAS detector at the LHC, Phys. Rev. Lett. **117**, 182002 (2016).

[31] S. Frixione, G. Ridolfi, and P. Nason, A positive-weight next-to-leading-order Monte Carlo for heavy flavour hadroproduction, J. High Energy Phys. 09 (2007) 126.

[32] T. Sjöstrand, S. Ask, J. R. Christiansen, R. Corke, N. Desai, P. Ilten, S. Mrenna, S. Prestel, C. O. Rasmussen, and P. Z. Skands, An introduction to Pythia 8.2, Comput. Phys. Commun. **191**, 159 (2015).

[33] ATLAS Collaboration, ATLAS Pythia8 tunes to 7 TeV data, Report No. ATL-PHYS-PUB-2014-021, 2014, https://cds.cern.ch/record/1966419.

[34] R. D. Ball *et al.* (NNPDF Collaboration), Parton distributions for the LHC Run II, J. High Energy Phys. 04 (2015) 040.

[35] ATLAS Collaboration, Studies on top-quark Monte Carlo modelling for Top2016, Report No. ATL-PHYS-PUB-2016-020, 2016, https://cds.cern.ch/record/2216168.

[36] J. Bellm *et al.*, Herwig 7.0/Herwig++ 3.0 release note, Eur. Phys. J. C **76**, 196 (2016).

[37] T. Ježo, J. M. Lindert, N. Moretti, and S. Pozzorini, New NLOPS predictions for $t\bar{t} + b$-jet production at the LHC, Eur. Phys. J. C **78**, 502 (2018).

[38] F. Buccioni, J.-N. Lang, J. M. Lindert, P. Maierhöfer, S. Pozzorini, H. Zhang, and M. F. Zoller, OpenLoops 2, Eur. Phys. J. C **79**, 866 (2019).

[39] F. Cascioli, P. Maierhöfer, and S. Pozzorini, Scattering amplitudes with open loops, Phys. Rev. Lett. **108**, 111601 (2012).

[40] A. Denner, S. Dittmaier, and L. Hofer, Collier: A Fortran-based complex one-loop library in extended regularizations, Comput. Phys. Commun. **212**, 220 (2017).

[41] T. Ježo, POWHEG-BOX-RES ttbb source code, https://gitlab.cern.ch/tjezo/powheg-box-res_ttbb/ (2019).

[42] R. Frederix, E. Re, and P. Torrielli, Single-top t-channel hadroproduction in the four-flavour scheme with POWHEG and aMC@NLO, J. High Energy Phys. 09 (2012) 130.
[43] S. Alioli, P. Nason, C. Oleari, and E. Re, NLO single-top production matched with shower in POWHEG: s- and t-channel contributions, J. High Energy Phys. 09 (2009) 111.
[44] E. Re, Single-top Wt-channel production matched with parton showers using the POWHEG method, Eur. Phys. J. C **71**, 1547 (2011).
[45] S. Frixione, E. Laenen, P. Motylinski, C. White, and B. R. Webber, Single-top hadroproduction in association with a W boson, J. High Energy Phys. 07 (2008) 029.
[46] J. Alwall, R. Frederix, S. Frixione, V. Hirschi, F. Maltoni, O. Mattelaer, H.-S. Shao, T. Stelzer, P. Torrielli, and M. Zaro, The automated computation of tree-level and next-to-leading order differential cross sections, and their matching to parton shower simulations, J. High Energy Phys. 07 (2014) 079.
[47] E. Bothmann *et al.*, Event generation with Sherpa 2.2, SciPost Phys. **7**, 034 (2019).
[48] T. Gleisberg and S. Höche, Comix, a new matrix element generator, J. High Energy Phys. 12 (2008) 039.
[49] S. Schumann and F. Krauss, A parton shower algorithm based on Catani-Seymour dipole factorisation, J. High Energy Phys. 03 (2008) 038.
[50] S. Höche, F. Krauss, M. Schönherr, and F. Siegert, A critical appraisal of NLO + PS matching methods, J. High Energy Phys. 09 (2012) 049.
[51] S. Höche, F. Krauss, M. Schönherr, and F. Siegert, QCD matrix elements + parton showers. The NLO case, J. High Energy Phys. 04 (2013) 027.
[52] S. Catani, F. Krauss, B. R. Webber, and R. Kuhn, QCD matrix elements + parton showers, J. High Energy Phys. 11 (2001) 063.
[53] S. Höche, F. Krauss, S. Schumann, and F. Siegert, QCD matrix elements and truncated showers, J. High Energy Phys. 05 (2009) 053.
[54] D. J. Lange, The EvtGen particle decay simulation package, Nucl. Instrum. Methods Phys. Res., Sect. A **462**, 152 (2001).
[55] ATLAS Collaboration, Early inner detector tracking performance in the 2015 data at $\sqrt{s} = 13$ TeV, Report No. ATL-PHYS-PUB-2015-051, 2015, https://cds.cern.ch/record/2110140.
[56] ATLAS Collaboration, Performance of the ATLAS track reconstruction algorithms in dense environments in LHC Run 2, Eur. Phys. J. C **77**, 673 (2017).
[57] ATLAS Collaboration, Vertex Reconstruction Performance of the ATLAS Detector at $\sqrt{s} = 13$ TeV, Report No. ATL-PHYS-PUB-2015-026, 2015, https://cds.cern.ch/record/2037717.
[58] P. Billoir and S. Qian, Fast vertex fitting with a local parametrization of tracks, Nucl. Instrum. Methods Phys. Res., Sect. A **311**, 139 (1992).
[59] ATLAS Collaboration, Electron and photon performance measurements with the ATLAS detector using the 2015–2017 LHC proton-proton collision data, J. Instrum. **14**, P12006 (2019).
[60] ATLAS Collaboration, Evidence for the associated production of the Higgs boson and a top quark pair with the ATLAS detector, Phys. Rev. D **97**, 072003 (2018).
[61] C. Magliocca, Measurement of the track impact parameters resolution with the ATLAS experiment at LHC using 2016–2018 data, Nuovo Cimento Soc. Ital. Fis. **44C**, 55 (2021).
[62] ATLAS Collaboration, Muon reconstruction and identification efficiency in ATLAS using the full Run 2 pp collision data set at $\sqrt{s} = 13$ TeV, Eur. Phys. J. C **81**, 578 (2021).
[63] ATLAS Collaboration, Jet reconstruction and performance using particle flow with the ATLAS detector, Eur. Phys. J. C **77**, 466 (2017).
[64] M. Cacciari, G. P. Salam, and G. Soyez, The anti-k_t jet clustering algorithm, J. High Energy Phys. 04 (2008) 063.
[65] M. Cacciari, G. P. Salam, and G. Soyez, FastJet user manual, Eur. Phys. J. C **72**, 1896 (2012).
[66] ATLAS Collaboration, Jet energy scale and resolution measured in proton-proton collisions at $\sqrt{s} = 13$ TeV with the ATLAS detector, Eur. Phys. J. C **81**, 689 (2021).
[67] ATLAS Collaboration, Performance of pile-up mitigation techniques for jets in pp collisions at $\sqrt{s} = 8$ TeV using the ATLAS detector, Eur. Phys. J. C **76**, 581 (2016).
[68] ATLAS Collaboration, The performance of missing transverse momentum reconstruction and its significance with the ATLAS detector using 140 fb^{-1} of $\sqrt{s} = 13$ TeV pp collisions, arXiv:2402.05858.
[69] ATLAS Collaboration, Flavor tagging with track-jets in boosted topologies with the ATLAS detector, Report No. ATL-PHYS-PUB-2014-013, 2014, https://cds.cern.ch/record/1750681.
[70] ATLAS Collaboration, Secondary vertex finding for jet flavour identification with the ATLAS detector, Report No. ATL-PHYS-PUB-2017-011, 2017, https://cds.cern.ch/record/2270366.
[71] ATLAS Collaboration, Measurement of the c-jet mistagging efficiency in $t\bar{t}$ events using pp collision data at $\sqrt{s} =$ 13 TeV collected with the ATLAS detector, Eur. Phys. J. C **82**, 95 (2022).
[72] ATLAS Collaboration, Calibration of the light-flavour jet mistagging efficiency of the b-tagging algorithms with $Z +$ jets events using 139 fb^{-1} of ATLAS proton–proton collision data at $\sqrt{s} = 13$ TeV, Eur. Phys. J. C **83**, 728 (2023).
[73] J. Butterworth *et al.*, PDF4LHC recommendations for LHC Run II, J. Phys. G **43**, 023001 (2016).
[74] ATLAS Collaboration, Measurement of Higgs boson decay into b-quarks in associated production with a top-quark pair in pp collisions at $\sqrt{s} = 13$ TeV with the ATLAS detector, J. High Energy Phys. 06 (2022) 097.
[75] ATLAS Collaboration, Search for new phenomena in events with two opposite-charge leptons, jets and missing transverse momentum in pp collisions at $\sqrt{s} = 13$ TeV with the ATLAS detector, J. High Energy Phys. 04 (2021) 165.
[76] ATLAS Collaboration, ATLAS computing acknowledgements, Report No. ATL-SOFT-PUB-2023-001, 2023, https://cds.cern.ch/record/2869272.

G. Aad,[104] E. Aakvaag,[17] B. Abbott,[123] S. Abdelhameed,[119a] K. Abeling,[56] N. J. Abicht,[50] S. H. Abidi,[30] M. Aboelela,[45] A. Aboulhorma,[36e] H. Abramowicz,[154] H. Abreu,[153] Y. Abulaiti,[120] B. S. Acharya,[70a,70b,b] A. Ackermann,[64a] C. Adam Bourdarios,[4] L. Adamczyk,[87a] S. V. Addepalli,[27] M. J. Addison,[103] J. Adelman,[118] A. Adiguzel,[22c] T. Adye,[137] A. A. Affolder,[139] Y. Afik,[40] M. N. Agaras,[13] J. Agarwala,[74a,74b] A. Aggarwal,[102] C. Agheorghiesei,[28c] F. Ahmadov,[39,c] W. S. Ahmed,[106] S. Ahuja,[97] X. Ai,[63e] G. Aielli,[77a,77b] A. Aikot,[166] M. Ait Tamlihat,[36e] B. Aitbenchikh,[36a] M. Akbiyik,[102] T. P. A. Åkesson,[100] A. V. Akimov,[38] D. Akiyama,[171] N. N. Akolkar,[25] S. Aktas,[22a] K. Al Khoury,[42] G. L. Alberghi,[24b] J. Albert,[168] P. Albicocco,[54] G. L. Albouy,[61] S. Alderweireldt,[53] Z. L. Alegria,[124] M. Aleksa,[37] I. N. Aleksandrov,[39] C. Alexa,[28b] T. Alexopoulos,[10] F. Alfonsi,[24b] M. Algren,[57] M. Alhroob,[170] B. Ali,[135] H. M. J. Ali,[93] S. Ali,[32] S. W. Alibocus,[94] M. Aliev,[34c] G. Alimonti,[72a] W. Alkakhi,[56] C. Allaire,[67] B. M. M. Allbrooke,[149] J. F. Allen,[53] C. A. Allendes Flores,[140f] P. P. Allport,[21] A. Aloisio,[73a,73b] F. Alonso,[92] C. Alpigiani,[141] Z. M. K. Alsolami,[93] M. Alvarez Estevez,[101] A. Alvarez Fernandez,[102] M. Alves Cardoso,[57] M. G. Alviggi,[73a,73b] M. Aly,[103] Y. Amaral Coutinho,[84b] A. Ambler,[106] C. Amelung,[37] M. Amerl,[103] C. G. Ames,[111] D. Amidei,[108] K. J. Amirie,[158] S. P. Amor Dos Santos,[133a] K. R. Amos,[166] S. An,[85] V. Ananiev,[128] C. Anastopoulos,[142] T. Andeen,[11] J. K. Anders,[37] A. C. Anderson,[60] S. Y. Andrean,[48a,48b] A. Andreazza,[72a,72b] S. Angelidakis,[9] A. Angerami,[42] A. V. Anisenkov,[38] A. Annovi,[75a] C. Antel,[57] E. Antipov,[148] M. Antonelli,[54] F. Anulli,[76a] M. Aoki,[85] T. Aoki,[156] M. A. Aparo,[149] L. Aperio Bella,[49] C. Appelt,[19] A. Apyan,[27] S. J. Arbiol Val,[88] C. Arcangeletti,[54] A. T. H. Arce,[52] E. Arena,[94] J-F. Arguin,[110] S. Argyropoulos,[55] J.-H. Arling,[49] O. Arnaez,[4] H. Arnold,[148] G. Artoni,[76a,76b] H. Asada,[113] K. Asai,[121] S. Asai,[156] N. A. Asbah,[37] R. A. Ashby Pickering,[170] K. Assamagan,[30] R. Astalos,[29a] K. S. V. Astrand,[100] S. Atashi,[162] R. J. Atkin,[34a] M. Atkinson,[165] H. Atmani,[36f] P. A. Atmasiddha,[131] K. Augsten,[135] S. Auricchio,[73a,73b] A. D. Auriol,[21] V. A. Austrup,[103] G. Avolio,[37] K. Axiotis,[57] G. Azuelos,[110,d] D. Babal,[29b] H. Bachacou,[138] K. Bachas,[155,e] A. Bachiu,[35] F. Backman,[48a,48b] A. Badea,[40] T. M. Baer,[108] P. Bagnaia,[76a,76b] M. Bahmani,[19] D. Bahner,[55] K. Bai,[126] J. T. Baines,[137] L. Baines,[96] O. K. Baker,[175] E. Bakos,[16] D. Bakshi Gupta,[8] L. E. Balabram Filho,[84b] V. Balakrishnan,[123] R. Balasubramanian,[117] E. M. Baldin,[38] P. Balek,[87a] E. Ballabene,[24b,24a] F. Balli,[138] L. M. Baltes,[64a] W. K. Balunas,[33] J. Balz,[102] I. Bamwidhi,[119b] E. Banas,[88] M. Bandieramonte,[132] A. Bandyopadhyay,[25] S. Bansal,[25] L. Barak,[154] M. Barakat,[49] E. L. Barberio,[107] D. Barberis,[58b,58a] M. Barbero,[104] M. Z. Barel,[117] K. N. Barends,[34a] T. Barillari,[112] M-S. Barisits,[37] T. Barklow,[146] P. Baron,[125] D. A. Baron Moreno,[103] A. Baroncelli,[63a] A. J. Barr,[129] J. D. Barr,[98] F. Barreiro,[101] J. Barreiro Guimarães da Costa,[14] U. Barron,[154] M. G. Barros Teixeira,[133a] S. Barsov,[38] F. Bartels,[64a] R. Bartoldus,[146] A. E. Barton,[93] P. Bartos,[29a] A. Basan,[102] M. Baselga,[50] A. Bassalat,[67,f] M. J. Basso,[159a] S. Bataju,[45] R. Bate,[167] R. L. Bates,[60] S. Batlamous,[101] B. Batool,[144] M. Battaglia,[139] D. Battulga,[19] M. Bauce,[76a,76b] M. Bauer,[80] P. Bauer,[25] L. T. Bazzano Hurrell,[31] J. B. Beacham,[52] T. Beau,[130] J. Y. Beaucamp,[92] P. H. Beauchemin,[161] P. Bechtle,[25] H. P. Beck,[20,g] K. Becker,[170] A. J. Beddall,[83] V. A. Bednyakov,[39] C. P. Bee,[148] L. J. Beemster,[16] T. A. Beermann,[37] M. Begalli,[84d] M. Begel,[30] A. Behera,[148] J. K. Behr,[49] J. F. Beirer,[37] F. Beisiegel,[25] M. Belfkir,[119b] G. Bella,[154] L. Bellagamba,[24b] A. Bellerive,[35] P. Bellos,[21] K. Beloborodov,[38] D. Benchekroun,[36a] F. Bendebba,[36a] Y. Benhammou,[154] K. C. Benkendorfer,[62] L. Beresford,[49] M. Beretta,[54] E. Bergeaas Kuutmann,[164] N. Berger,[4] B. Bergmann,[135] J. Beringer,[18a] G. Bernardi,[5] C. Bernius,[146] F. U. Bernlochner,[25] F. Bernon,[37,104] A. Berrocal Guardia,[13] T. Berry,[97] P. Berta,[136] A. Berthold,[51] S. Bethke,[112] A. Betti,[76a,76b] A. J. Bevan,[96] N. K. Bhalla,[55] S. Bhatta,[148] D. S. Bhattacharya,[169] P. Bhattarai,[146] K. D. Bhide,[55] V. S. Bhopatkar,[124] R. M. Bianchi,[132] G. Bianco,[24b,24a] O. Biebel,[111] R. Bielski,[126] M. Biglietti,[78a] C. S. Billingsley,[45] M. Bindi,[56] A. Bingul,[22b] C. Bini,[76a,76b] A. Biondini,[94] G. A. Bird,[33] M. Birman,[172] M. Biros,[136] S. Biryukov,[149] T. Bisanz,[50] E. Bisceglie,[44b,44a] J. P. Biswal,[137] D. Biswas,[144] I. Bloch,[49] A. Blue,[60] U. Blumenschein,[96] J. Blumenthal,[102] V. S. Bobrovnikov,[38] M. Boehler,[55] B. Boehm,[169] D. Bogavac,[37] A. G. Bogdanchikov,[38] C. Bohm,[48a] V. Boisvert,[97] P. Bokan,[37] T. Bold,[87a] M. Bomben,[5] M. Bona,[96] M. Boonekamp,[138] C. D. Booth,[97] A. G. Borbély,[60] I. S. Bordulev,[38] H. M. Borecka-Bielska,[110] G. Borissov,[93] D. Bortoletto,[129] D. Boscherini,[24b] M. Bosman,[13] J. D. Bossio Sola,[37] K. Bouaouda,[36a] N. Bouchhar,[166] L. Boudet,[4] J. Boudreau,[132] E. V. Bouhova-Thacker,[93] D. Boumediene,[41] R. Bouquet,[58b,58a] A. Boveia,[122] J. Boyd,[37] D. Boye,[30] I. R. Boyko,[39] L. Bozianu,[57] J. Bracinik,[21] N. Brahimi,[4] G. Brandt,[174] O. Brandt,[33] F. Braren,[49] B. Brau,[105] J. E. Brau,[126] R. Brener,[172] L. Brenner,[117] R. Brenner,[164]

S. Bressler,[172] G. Brianti,[79a,79b] D. Britton,[60] D. Britzger,[112] I. Brock,[25] G. Brooijmans,[42] E. M. Brooks,[159b] E. Brost,[30] L. M. Brown,[168] L. E. Bruce,[62] T. L. Bruckler,[129] P. A. Bruckman de Renstrom,[88] B. Brüers,[49] A. Bruni,[24b] G. Bruni,[24b] M. Bruschi,[24b] N. Bruscino,[76a,76b] T. Buanes,[17] Q. Buat,[141] D. Buchin,[112] A. G. Buckley,[60] O. Bulekov,[38] B. A. Bullard,[146] S. Burdin,[94] C. D. Burgard,[50] A. M. Burger,[37] B. Burghgrave,[8] O. Burlayenko,[55] J. Burleson,[165] J. T. P. Burr,[33] J. C. Burzynski,[145] E. L. Busch,[42] V. Büscher,[102] P. J. Bussey,[60] J. M. Butler,[26] C. M. Buttar,[60] J. M. Butterworth,[98] W. Buttinger,[137] C. J. Buxo Vazquez,[109] A. R. Buzykaev,[38] S. Cabrera Urbán,[166] L. Cadamuro,[67] D. Caforio,[59] H. Cai,[132] Y. Cai,[14,114c] Y. Cai,[114a] V. M. M. Cairo,[37] O. Cakir,[3a] N. Calace,[37] P. Calafiura,[18a] G. Calderini,[130] P. Calfayan,[69] G. Callea,[60] L. P. Caloba,[84b] D. Calvet,[41] S. Calvet,[41] M. Calvetti,[75a,75b] R. Camacho Toro,[130] S. Camarda,[37] D. Camarero Munoz,[27] P. Camarri,[77a,77b] M. T. Camerlingo,[73a,73b] D. Cameron,[37] C. Camincher,[168] M. Campanelli,[98] A. Camplani,[43] V. Canale,[73a,73b] A. C. Canbay,[3a] E. Canonero,[97] J. Cantero,[166] Y. Cao,[165] F. Capocasa,[27] M. Capua,[44b,44a] A. Carbone,[72a,72b] R. Cardarelli,[77a] J. C. J. Cardenas,[8] G. Carducci,[44b,44a] T. Carli,[37] G. Carlino,[73a] J. I. Carlotto,[13] B. T. Carlson,[132,h] E. M. Carlson,[168,159a] J. Carmignani,[94] L. Carminati,[72a,72b] A. Carnelli,[138] M. Carnesale,[76a,76b] S. Caron,[116] E. Carquin,[140f] S. Carrá,[72a] G. Carratta,[24b,24a] A. M. Carroll,[126] T. M. Carter,[53] M. P. Casado,[13,i] M. Caspar,[49] F. L. Castillo,[4] L. Castillo Garcia,[13] V. Castillo Gimenez,[166] N. F. Castro,[133a,133e] A. Catinaccio,[37] J. R. Catmore,[128] T. Cavaliere,[4] V. Cavaliere,[30] N. Cavalli,[24b,24a] L. J. Caviedes Betancourt,[23b] Y. C. Cekmecelioglu,[49] E. Celebi,[83] S. Cella,[37] F. Celli,[129] M. S. Centonze,[71a,71b] V. Cepaitis,[57] K. Cerny,[125] A. S. Cerqueira,[84a] A. Cerri,[149] L. Cerrito,[77a,77b] F. Cerutti,[18a] B. Cervato,[144] A. Cervelli,[24b] G. Cesarini,[54] S. A. Cetin,[83] D. Chakraborty,[118] J. Chan,[18a] W. Y. Chan,[156] J. D. Chapman,[33] E. Chapon,[138] B. Chargeishvili,[152b] D. G. Charlton,[21] M. Chatterjee,[20] C. Chauhan,[136] Y. Che,[114a] S. Chekanov,[6] S. V. Chekulaev,[159a] G. A. Chelkov,[39,j] A. Chen,[108] B. Chen,[154] B. Chen,[168] H. Chen,[114a] H. Chen,[30] J. Chen,[63c] J. Chen,[145] M. Chen,[129] S. Chen,[156] S. J. Chen,[114a] X. Chen,[63c,138] X. Chen,[15,k] Y. Chen,[63a] C. L. Cheng,[173] H. C. Cheng,[65a] S. Cheong,[146] A. Cheplakov,[39] E. Cheremushkina,[49] E. Cherepanova,[117] R. Cherkaoui El Moursli,[36e] E. Cheu,[7] K. Cheung,[66] L. Chevalier,[138] V. Chiarella,[54] G. Chiarelli,[75a] N. Chiedde,[104] G. Chiodini,[71a] A. S. Chisholm,[21] A. Chitan,[28b] M. Chitishvili,[166] M. V. Chizhov,[39] K. Choi,[11] Y. Chou,[141] E. Y. S. Chow,[116] K. L. Chu,[172] M. C. Chu,[65a] X. Chu,[14,114c] Z. Chubinidze,[54] J. Chudoba,[134] J. J. Chwastowski,[88] D. Cieri,[112] K. M. Ciesla,[87a] V. Cindro,[95] A. Ciocio,[18a] F. Cirotto,[73a,73b] Z. H. Citron,[172] M. Citterio,[72a] D. A. Ciubotaru,[28b] A. Clark,[57] P. J. Clark,[53] N. Clarke Hall,[98] C. Clarry,[158] J. M. Clavijo Columbie,[49] S. E. Clawson,[49] C. Clement,[48a,48b] Y. Coadou,[104] M. Cobal,[70a,70c] A. Coccaro,[58b] R. F. Coelho Barrue,[133a] R. Coelho Lopes De Sa,[105] S. Coelli,[72a] B. Cole,[42] J. Collot,[61] P. Conde Muiño,[133a,133g] M. P. Connell,[34c] S. H. Connell,[34c] E. I. Conroy,[129] F. Conventi,[73a,l] H. G. Cooke,[21] A. M. Cooper-Sarkar,[129] F. A. Corchia,[24b,24a] A. Cordeiro Oudot Choi,[130] L. D. Corpe,[41] M. Corradi,[76a,76b] F. Corriveau,[106,m] A. Cortes-Gonzalez,[19] M. J. Costa,[166] F. Costanza,[4] D. Costanzo,[142] B. M. Cote,[122] J. Couthures,[4] G. Cowan,[97] K. Cranmer,[173] D. Cremonini,[24b,24a] S. Crépé-Renaudin,[61] F. Crescioli,[130] M. Cristinziani,[144] M. Cristoforetti,[79a,79b] V. Croft,[117] J. E. Crosby,[124] G. Crosetti,[44b,44a] A. Cueto,[101] H. Cui,[98] Z. Cui,[7] W. R. Cunningham,[60] F. Curcio,[166] J. R. Curran,[53] P. Czodrowski,[37] M. M. Czurylo,[37] M. J. Da Cunha Sargedas De Sousa,[58b,58a] J. V. Da Fonseca Pinto,[84b] C. Da Via,[103] W. Dabrowski,[87a] T. Dado,[50] S. Dahbi,[151] T. Dai,[108] D. Dal Santo,[20] C. Dallapiccola,[105] M. Dam,[43] G. D'amen,[30] V. D'Amico,[111] J. Damp,[102] J. R. Dandoy,[35] D. Dannheim,[37] M. Danninger,[145] V. Dao,[148] G. Darbo,[58b] S. J. Das,[30,n] F. Dattola,[49] S. D'Auria,[72a,72b] A. D'avanzo,[73a,73b] C. David,[34a] T. Davidek,[136] I. Dawson,[96] H. A. Day-hall,[135] K. De,[8] R. De Asmundis,[73a] N. De Biase,[49] S. De Castro,[24b,24a] N. De Groot,[116] P. de Jong,[117] H. De la Torre,[118] A. De Maria,[114a] A. De Salvo,[76a] U. De Sanctis,[77a,77b] F. De Santis,[71a,71b] A. De Santo,[149] J. B. De Vivie De Regie,[61] D. V. Dedovich,[39] J. Degens,[94] A. M. Deiana,[45] F. Del Corso,[24b,24a] J. Del Peso,[101] F. Del Rio,[64a] L. Delagrange,[130] F. Deliot,[138] C. M. Delitzsch,[50] M. Della Pietra,[73a,73b] D. Della Volpe,[57] A. Dell'Acqua,[37] L. Dell'Asta,[72a,72b] M. Delmastro,[4] P. A. Delsart,[61] S. Demers,[175] M. Demichev,[39] S. P. Denisov,[38] L. D'Eramo,[41] D. Derendarz,[88] F. Derue,[130] P. Dervan,[94] K. Desch,[25] C. Deutsch,[25] F. A. Di Bello,[58b,58a] A. Di Ciaccio,[77a,77b] L. Di Ciaccio,[4] A. Di Domenico,[76a,76b] C. Di Donato,[73a,73b] A. Di Girolamo,[37] G. Di Gregorio,[37] A. Di Luca,[79a,79b] B. Di Micco,[78a,78b] R. Di Nardo,[78a,78b] K. F. Di Petrillo,[40] M. Diamantopoulou,[35] F. A. Dias,[117] T. Dias Do Vale,[145] M. A. Diaz,[140a,140b] F. G. Diaz Capriles,[25]

A. R. Didenko,[39] M. Didenko,[166] E. B. Diehl,[108] S. Díez Cornell,[49] C. Diez Pardos,[144] C. Dimitriadi,[164] A. Dimitrievska,[21] J. Dingfelder,[25] T. Dingley,[129] I-M. Dinu,[28b] S. J. Dittmeier,[64b] F. Dittus,[37] M. Divisek,[136] F. Djama,[104] T. Djobava,[152b] C. Doglioni,[103,100] A. Dohnalova,[29a] J. Dolejsi,[136] Z. Dolezal,[136] K. Domijan,[87a] K. M. Dona,[40] M. Donadelli,[84d] B. Dong,[109] J. Donini,[41] A. D'Onofrio,[73a,73b] M. D'Onofrio,[94] J. Dopke,[137] A. Doria,[73a] N. Dos Santos Fernandes,[133a] P. Dougan,[103] M. T. Dova,[92] A. T. Doyle,[60] M. A. Draguet,[129] E. Dreyer,[172] I. Drivas-koulouris,[10] M. Drnevich,[120] M. Drozdova,[57] D. Du,[63a] T. A. du Pree,[117] F. Dubinin,[38] M. Dubovsky,[29a] E. Duchovni,[172] G. Duckeck,[111] O. A. Ducu,[28b] D. Duda,[53] A. Dudarev,[37] E. R. Duden,[27] M. D'uffizi,[103] L. Duflot,[67] M. Dührssen,[37] I. Duminica,[28g] A. E. Dumitriu,[28b] M. Dunford,[64a] S. Dungs,[50] K. Dunne,[48a,48b] A. Duperrin,[104] H. Duran Yildiz,[3a] M. Düren,[59] A. Durglishvili,[152b] B. L. Dwyer,[118] G. I. Dyckes,[18a] M. Dyndal,[87a] B. S. Dziedzic,[37] Z. O. Earnshaw,[149] G. H. Eberwein,[129] B. Eckerova,[29a] S. Eggebrecht,[56] E. Egidio Purcino De Souza,[130] L. F. Ehrke,[57] G. Eigen,[17] K. Einsweiler,[18a] T. Ekelof,[164] P. A. Ekman,[100] S. El Farkh,[36b] Y. El Ghazali,[63a] H. El Jarrari,[37] A. El Moussaouy,[36a] V. Ellajosyula,[164] M. Ellert,[164] F. Ellinghaus,[174] N. Ellis,[37] J. Elmsheuser,[30] M. Elsawy,[119a] M. Elsing,[37] D. Emeliyanov,[137] Y. Enari,[156] I. Ene,[18a] S. Epari,[13] P. A. Erland,[88] D. Ernani Martins Neto,[88] M. Errenst,[174] M. Escalier,[67] C. Escobar,[166] E. Etzion,[154] G. Evans,[133a] H. Evans,[69] L. S. Evans,[97] A. Ezhilov,[38] S. Ezzarqtouni,[36a] F. Fabbri,[24b,24a] L. Fabbri,[24b,24a] G. Facini,[98] V. Fadeyev,[139] R. M. Fakhrutdinov,[38] D. Fakoudis,[102] S. Falciano,[76a] L. F. Falda Ulhoa Coelho,[37] F. Fallavollita,[112] G. Falsetti,[44b,44a] J. Faltova,[136] C. Fan,[165] Y. Fan,[14] Y. Fang,[14,114c] M. Fanti,[72a,72b] M. Faraj,[70a,70b] Z. Farazpay,[99] A. Farbin,[8] A. Farilla,[78a] T. Farooque,[109] S. M. Farrington,[53] F. Fassi,[36e] D. Fassouliotis,[9] M. Faucci Giannelli,[77a,77b] W. J. Fawcett,[33] L. Fayard,[67] P. Federic,[136] P. Federicova,[134] O. L. Fedin,[38,j] M. Feickert,[173] L. Feligioni,[104] D. E. Fellers,[126] C. Feng,[63b] M. Feng,[15] Z. Feng,[117] M. J. Fenton,[162] L. Ferencz,[49] R. A. M. Ferguson,[93] S. I. Fernandez Luengo,[140f] P. Fernandez Martinez,[13] M. J. V. Fernoux,[104] J. Ferrando,[93] A. Ferrari,[164] P. Ferrari,[117,116] R. Ferrari,[74a] D. Ferrere,[57] C. Ferretti,[108] D. Fiacco,[76a,76b] F. Fiedler,[102] P. Fiedler,[135] A. Filipčič,[95] E. K. Filmer,[1] F. Filthaut,[116] M. C. N. Fiolhais,[133a,133c,o] L. Fiorini,[166] W. C. Fisher,[109] T. Fitschen,[103] P. M. Fitzhugh,[138] I. Fleck,[144] P. Fleischmann,[108] T. Flick,[174] M. Flores,[34d,p] L. R. Flores Castillo,[65a] L. Flores Sanz De Acedo,[37] F. M. Follega,[79a,79b] N. Fomin,[33] J. H. Foo,[158] A. Formica,[138] A. C. Forti,[103] E. Fortin,[37] A. W. Fortman,[18a] M. G. Foti,[18a] L. Fountas,[9,q] D. Fournier,[67] H. Fox,[93] P. Francavilla,[75a,75b] S. Francescato,[62] S. Franchellucci,[57] M. Franchini,[24b,24a] S. Franchino,[64a] D. Francis,[37] L. Franco,[116] V. Franco Lima,[37] L. Franconi,[49] M. Franklin,[62] G. Frattari,[27] Y. Y. Frid,[154] J. Friend,[60] N. Fritzsche,[51] A. Froch,[55] D. Froidevaux,[37] J. A. Frost,[129] Y. Fu,[63a] S. Fuenzalida Garrido,[140f] M. Fujimoto,[104] K. Y. Fung,[65a] E. Furtado De Simas Filho,[84e] M. Furukawa,[156] J. Fuster,[166] A. Gaa,[56] A. Gabrielli,[24b,24a] A. Gabrielli,[158] P. Gadow,[37] G. Gagliardi,[58b,58a] L. G. Gagnon,[18a] S. Gaid,[163] S. Galantzan,[154] E. J. Gallas,[129] B. J. Gallop,[137] K. K. Gan,[122] S. Ganguly,[156] Y. Gao,[53] F. M. Garay Walls,[140a,140b] B. Garcia,[30] C. García,[166] A. Garcia Alonso,[117] A. G. Garcia Caffaro,[175] J. E. García Navarro,[166] M. Garcia-Sciveres,[18a] G. L. Gardner,[131] R. W. Gardner,[40] N. Garelli,[161] D. Garg,[81] R. B. Garg,[146] J. M. Gargan,[53] C. A. Garner,[158] C. M. Garvey,[34a] V. K. Gassmann,[161] G. Gaudio,[74a] V. Gautam,[13] P. Gauzzi,[76a,76b] J. Gavranovic,[95] I. L. Gavrilenko,[38] A. Gavrilyuk,[38] C. Gay,[167] G. Gaycken,[126] E. N. Gazis,[10] A. A. Geanta,[28b] C. M. Gee,[139] A. Gekow,[122] C. Gemme,[58b] M. H. Genest,[61] A. D. Gentry,[115] S. George,[97] W. F. George,[21] T. Geralis,[47] P. Gessinger-Befurt,[37] M. E. Geyik,[174] M. Ghani,[170] K. Ghorbanian,[96] A. Ghosal,[144] A. Ghosh,[162] A. Ghosh,[7] B. Giacobbe,[24b] S. Giagu,[76a,76b] T. Giani,[117] A. Giannini,[63a] S. M. Gibson,[97] M. Gignac,[139] D. T. Gil,[87b] A. K. Gilbert,[87a] B. J. Gilbert,[42] D. Gillberg,[35] G. Gilles,[117] L. Ginabat,[130] D. M. Gingrich,[2,d] M. P. Giordani,[70a,70c] P. F. Giraud,[138] G. Giugliarelli,[70a,70c] D. Giugni,[72a] F. Giuli,[37] I. Gkialas,[9,q] L. K. Gladilin,[38] C. Glasman,[101] G. R. Gledhill,[126] G. Glemža,[49] M. Glisic,[126] I. Gnesi,[44b,r] Y. Go,[30] M. Goblirsch-Kolb,[37] B. Gocke,[50] D. Godin,[110] B. Gokturk,[22a] S. Goldfarb,[107] T. Golling,[57] M. G. D. Gololo,[34g] D. Golubkov,[38] J. P. Gombas,[109] A. Gomes,[133a,133b] G. Gomes Da Silva,[144] A. J. Gomez Delegido,[166] R. Gonçalo,[133a] L. Gonella,[21] A. Gongadze,[152c] F. Gonnella,[21] J. L. Gonski,[146] R. Y. González Andana,[53] S. González de la Hoz,[166] R. Gonzalez Lopez,[94] C. Gonzalez Renteria,[18a] M. V. Gonzalez Rodrigues,[49] R. Gonzalez Suarez,[164] S. Gonzalez-Sevilla,[57] L. Goossens,[37] B. Gorini,[37] E. Gorini,[71a,71b] A. Gorišek,[95] T. C. Gosart,[131] A. T. Goshaw,[52] M. I. Gostkin,[39] S. Goswami,[124] C. A. Gottardo,[37] S. A. Gotz,[111] M. Gouighri,[36b] V. Goumarre,[49] A. G. Goussiou,[141] N. Govender,[34c]

I. Grabowska-Bold,[87a] K. Graham,[35] E. Gramstad,[128] S. Grancagnolo,[71a,71b] C. M. Grant,[1,138] P. M. Gravila,[28f] F. G. Gravili,[71a,71b] H. M. Gray,[18a] M. Greco,[71a,71b] M. J. Green,[1] C. Grefe,[25] A. S. Grefsrud,[17] I. M. Gregor,[49] K. T. Greif,[162] P. Grenier,[146] S. G. Grewe,[112] A. A. Grillo,[139] K. Grimm,[32] S. Grinstein,[13,s] J.-F. Grivaz,[67] E. Gross,[172] J. Grosse-Knetter,[56] J. C. Grundy,[129] L. Guan,[108] J. G. R. Guerrero Rojas,[166] G. Guerrieri,[70a,70c] R. Gugel,[102] J. A. M. Guhit,[108] A. Guida,[19] E. Guilloton,[170] S. Guindon,[37] F. Guo,[14,114c] J. Guo,[63c] L. Guo,[49] Y. Guo,[108] R. Gupta,[132] S. Gurbuz,[25] S. S. Gurdasani,[55] G. Gustavino,[76a,76b] P. Gutierrez,[123] L. F. Gutierrez Zagazeta,[131] M. Gutsche,[51] C. Gutschow,[98] C. Gwenlan,[129] C. B. Gwilliam,[94] E. S. Haaland,[128] A. Haas,[120] M. Habedank,[49] C. Haber,[18a] H. K. Hadavand,[8] A. Hadef,[51] S. Hadzic,[112] A. I. Hagan,[93] J. J. Hahn,[144] E. H. Haines,[98] M. Haleem,[169] J. Haley,[124] J. J. Hall,[142] G. D. Hallewell,[104] L. Halser,[20] K. Hamano,[168] M. Hamer,[25] G. N. Hamity,[53] E. J. Hampshire,[97] J. Han,[63b] K. Han,[63a] L. Han,[114a] L. Han,[63a] S. Han,[18a] Y. F. Han,[158] K. Hanagaki,[85] M. Hance,[139] D. A. Hangal,[42] H. Hanif,[145] M. D. Hank,[131] J. B. Hansen,[43] P. H. Hansen,[43] K. Hara,[160] D. Harada,[57] T. Harenberg,[174] S. Harkusha,[38] M. L. Harris,[105] Y. T. Harris,[129] J. Harrison,[13] N. M. Harrison,[122] P. F. Harrison,[170] N. M. Hartman,[112] N. M. Hartmann,[111] R. Z. Hasan,[97,137] Y. Hasegawa,[143] S. Hassan,[17] R. Hauser,[109] C. M. Hawkes,[21] R. J. Hawkings,[37] Y. Hayashi,[156] S. Hayashida,[113] D. Hayden,[109] C. Hayes,[108] R. L. Hayes,[117] C. P. Hays,[129] J. M. Hays,[96] H. S. Hayward,[94] F. He,[63a] M. He,[14,114c] Y. He,[157] Y. He,[49] Y. He,[98] N. B. Heatley,[96] V. Hedberg,[100] A. L. Heggelund,[128] N. D. Hehir,[96,a] C. Heidegger,[55] K. K. Heidegger,[55] J. Heilman,[35] S. Heim,[49] T. Heim,[18a] J. G. Heinlein,[131] J. J. Heinrich,[126] L. Heinrich,[112,t] J. Hejbal,[134] A. Held,[173] S. Hellesund,[17] C. M. Helling,[167] S. Hellman,[48a,48b] R. C. W. Henderson,[93] L. Henkelmann,[33] A. M. Henriques Correia,[37] H. Herde,[100] Y. Hernández Jiménez,[148] L. M. Herrmann,[25] T. Herrmann,[51] G. Herten,[55] R. Hertenberger,[111] L. Hervas,[37] M. E. Hesping,[102] N. P. Hessey,[159a] M. Hidaoui,[36b] N. Hidic,[136] E. Hill,[158] S. J. Hillier,[21] J. R. Hinds,[109] F. Hinterkeuser,[25] M. Hirose,[127] S. Hirose,[160] D. Hirschbuehl,[174] T. G. Hitchings,[103] B. Hiti,[95] J. Hobbs,[148] R. Hobincu,[28e] N. Hod,[172] M. C. Hodgkinson,[142] B. H. Hodkinson,[129] A. Hoecker,[37] D. D. Hofer,[108] J. Hofer,[49] T. Holm,[25] M. Holzbock,[112] L. B. A. H. Hommels,[33] B. P. Honan,[103] J. J. Hong,[69] J. Hong,[63c] T. M. Hong,[132] B. H. Hooberman,[165] W. H. Hopkins,[6] M. C. Hoppesch,[165] Y. Horii,[113] S. Hou,[151] A. S. Howard,[95] J. Howarth,[60] J. Hoya,[6] M. Hrabovsky,[125] A. Hrynevich,[49] T. Hryn'ova,[4] P. J. Hsu,[66] S.-C. Hsu,[141] T. Hsu,[67] M. Hu,[18a] Q. Hu,[63a] S. Huang,[65b] X. Huang,[14,114c] Y. Huang,[142] Y. Huang,[102] Y. Huang,[14] Z. Huang,[103] Z. Hubacek,[135] M. Huebner,[25] F. Huegging,[25] T. B. Huffman,[129] C. A. Hugli,[49] M. Huhtinen,[37] S. K. Huiberts,[17] R. Hulsken,[106] N. Huseynov,[12,u] J. Huston,[109] J. Huth,[62] R. Hyneman,[146] G. Iacobucci,[57] G. Iakovidis,[30] L. Iconomidou-Fayard,[67] J. P. Iddon,[37] P. Iengo,[73a,73b] R. Iguchi,[156] Y. Iiyama,[156] T. Iizawa,[129] Y. Ikegami,[85] N. Ilic,[158] H. Imam,[84c] M. Ince Lezki,[57] T. Ingebretsen Carlson,[48a,48b] J. M. Inglis,[96] G. Introzzi,[74a,74b] M. Iodice,[78a] V. Ippolito,[76a,76b] R. K. Irwin,[94] M. Ishino,[156] W. Islam,[173] C. Issever,[19,49] S. Istin,[22a,v] H. Ito,[171] R. Iuppa,[79a,79b] A. Ivina,[172] J. M. Izen,[46] V. Izzo,[73a] P. Jacka,[134] P. Jackson,[1] C. S. Jagfeld,[111] G. Jain,[159a] P. Jain,[49] K. Jakobs,[55] T. Jakoubek,[172] J. Jamieson,[60] W. Jang,[156] M. Javurkova,[105] P. Jawahar,[103] L. Jeanty,[126] J. Jejelava,[152a,w] P. Jenni,[55,x] C. E. Jessiman,[35] C. Jia,[63b] J. Jia,[148] X. Jia,[62] X. Jia,[14,114c] Z. Jia,[114a] C. Jiang,[53] S. Jiggins,[49] J. Jimenez Pena,[13] S. Jin,[114a] A. Jinaru,[28b] O. Jinnouchi,[157] P. Johansson,[142] K. A. Johns,[7] J. W. Johnson,[139] D. M. Jones,[149] E. Jones,[49] P. Jones,[33] R. W. L. Jones,[93] T. J. Jones,[94] H. L. Joos,[56,37] R. Joshi,[122] J. Jovicevic,[16] X. Ju,[18a] J. J. Junggeburth,[105] T. Junkermann,[64a] A. Juste Rozas,[13,s] M. K. Juzek,[88] S. Kabana,[140e] A. Kaczmarska,[88] M. Kado,[112] H. Kagan,[122] M. Kagan,[146] A. Kahn,[131] C. Kahra,[102] T. Kaji,[156] E. Kajomovitz,[153] N. Kakati,[172] I. Kalaitzidou,[55] C. W. Kalderon,[30] N. J. Kang,[139] D. Kar,[34g] K. Karava,[129] M. J. Kareem,[159b] E. Karentzos,[55] O. Karkout,[117] S. N. Karpov,[39] Z. M. Karpova,[39] V. Kartvelishvili,[93] A. N. Karyukhin,[38] E. Kasimi,[155] J. Katzy,[49] S. Kaur,[35] K. Kawade,[143] M. P. Kawale,[123] C. Kawamoto,[89] T. Kawamoto,[63a] E. F. Kay,[37] F. I. Kaya,[161] S. Kazakos,[109] V. F. Kazanin,[38] Y. Ke,[148] J. M. Keaveney,[34a] R. Keeler,[168] G. V. Kehris,[62] J. S. Keller,[35] A. S. Kelly,[98] J. J. Kempster,[149] P. D. Kennedy,[102] O. Kepka,[134] B. P. Kerridge,[137] S. Kersten,[174] B. P. Kerševan,[95] L. Keszeghova,[29a] S. Ketabchi Haghighat,[158] R. A. Khan,[132] A. Khanov,[124] A. G. Kharlamov,[38] T. Kharlamova,[38] E. E. Khoda,[141] M. Kholodenko,[38] T. J. Khoo,[19] G. Khoriauli,[169] J. Khubua,[152b,a] Y. A. R. Khwaira,[130] B. Kibirige,[34g] D. Kim,[6] D. W. Kim,[48a,48b] Y. K. Kim,[40] N. Kimura,[98] M. K. Kingston,[56] A. Kirchhoff,[56] C. Kirfel,[25] F. Kirfel,[25] J. Kirk,[137] A. E. Kiryunin,[112] C. Kitsaki,[10] O. Kivernyk,[25] M. Klassen,[161] C. Klein,[35] L. Klein,[169] M. H. Klein,[45] S. B. Klein,[57] U. Klein,[94]

P. Klimek,[37] A. Klimentov,[30] T. Klioutchnikova,[37] P. Kluit,[117] S. Kluth,[112] E. Kneringer,[80] T. M. Knight,[158] A. Knue,[50] R. Kobayashi,[89] D. Kobylianskii,[172] S. F. Koch,[129] M. Kocian,[146] P. Kodyš,[136] D. M. Koeck,[126] P. T. Koenig,[25] T. Koffas,[35] O. Kolay,[51] I. Koletsou,[4] T. Komarek,[88] K. Köneke,[55] A. X. Y. Kong,[1] T. Kono,[121] N. Konstantinidis,[98] P. Kontaxakis,[57] B. Konya,[100] R. Kopeliansky,[42] S. Koperny,[87a] K. Korcyl,[88] K. Kordas,[155,y] A. Korn,[98] S. Korn,[56] I. Korolkov,[13] N. Korotkova,[38] B. Kortman,[117] O. Kortner,[112] S. Kortner,[112] W. H. Kostecka,[118] V. V. Kostyukhin,[144] A. Kotsokechagia,[138] A. Kotwal,[52] A. Koulouris,[37] A. Kourkoumeli-Charalampidi,[74a,74b] C. Kourkoumelis,[9] E. Kourlitis,[112,t] O. Kovanda,[126] R. Kowalewski,[168] W. Kozanecki,[138] A. S. Kozhin,[38] V. A. Kramarenko,[38] G. Kramberger,[95] P. Kramer,[102] M. W. Krasny,[130] A. Krasznahorkay,[37] A. C. Kraus,[118] J. W. Kraus,[174] J. A. Kremer,[49] T. Kresse,[51] L. Kretschmann,[174] J. Kretzschmar,[94] K. Kreul,[19] P. Krieger,[158] S. Krishnamurthy,[105] M. Krivos,[136] K. Krizka,[21] K. Kroeninger,[50] H. Kroha,[112] J. Kroll,[134] J. Kroll,[131] K. S. Krowpman,[109] U. Kruchonak,[39] H. Krüger,[25] N. Krumnack,[82] M. C. Kruse,[52] O. Kuchinskaia,[38] S. Kuday,[3a] S. Kuehn,[37] R. Kuesters,[55] T. Kuhl,[49] V. Kukhtin,[39] Y. Kulchitsky,[38,j] S. Kuleshov,[140d,140b] M. Kumar,[34g] N. Kumari,[49] P. Kumari,[159b] A. Kupco,[134] T. Kupfer,[50] A. Kupich,[38] O. Kuprash,[55] H. Kurashige,[86] L. L. Kurchaninov,[159a] O. Kurdysh,[67] Y. A. Kurochkin,[38] A. Kurova,[38] M. Kuze,[157] A. K. Kvam,[105] J. Kvita,[125] T. Kwan,[106] N. G. Kyriacou,[108] L. A. O. Laatu,[104] C. Lacasta,[166] F. Lacava,[76a,76b] H. Lacker,[19] D. Lacour,[130] N. N. Lad,[98] E. Ladygin,[39] A. Lafarge,[41] B. Laforge,[130] T. Lagouri,[175] F. Z. Lahbabi,[36a] S. Lai,[56] J. E. Lambert,[168] S. Lammers,[69] W. Lampl,[7] C. Lampoudis,[155,y] G. Lamprinoudis,[102] A. N. Lancaster,[118] E. Lançon,[30] U. Landgraf,[55] M. P. J. Landon,[96] V. S. Lang,[55] O. K. B. Langrekken,[128] A. J. Lankford,[162] F. Lanni,[37] K. Lantzsch,[25] A. Lanza,[74a] J. F. Laporte,[138] T. Lari,[72a] F. Lasagni Manghi,[24b] M. Lassnig,[37] V. Latonova,[134] A. Laurier,[153] S. D. Lawlor,[142] Z. Lawrence,[103] R. Lazaridou,[170] M. Lazzaroni,[72a,72b] B. Le,[103] E. M. Le Boulicaut,[52] L. T. Le Pottier,[18a] B. Leban,[24b,24a] A. Lebedev,[82] M. LeBlanc,[103] F. Ledroit-Guillon,[61] S. C. Lee,[151] S. Lee,[48a,48b] T. F. Lee,[94] L. L. Leeuw,[34c] H. P. Lefebvre,[97] M. Lefebvre,[168] C. Leggett,[18a] G. Lehmann Miotto,[37] M. Leigh,[57] W. A. Leight,[105] W. Leinonen,[116] A. Leisos,[155,z] M. A. L. Leite,[84c] C. E. Leitgeb,[19] R. Leitner,[136] K. J. C. Leney,[45] T. Lenz,[25] S. Leone,[75a] C. Leonidopoulos,[53] A. Leopold,[147] R. Les,[109] C. G. Lester,[33] M. Levchenko,[38] J. Levêque,[4] L. J. Levinson,[172] G. Levrini,[24b,24a] M. P. Lewicki,[88] C. Lewis,[141] D. J. Lewis,[4] A. Li,[5] B. Li,[63b] C. Li,[63a] C-Q. Li,[112] H. Li,[63a] H. Li,[63b] H. Li,[63b] H. Li,[114a] H. Li,[15] H. Li,[63b] J. Li,[63c] K. Li,[141] L. Li,[63c] M. Li,[14,114c] S. Li,[14,114c] S. Li,[63d,63c] T. Li,[5] X. Li,[106] Z. Li,[129] Z. Li,[156] Z. Li,[14,114c] Z. Li,[63a] S. Liang,[14,114c] Z. Liang,[14] M. Liberatore,[138] B. Liberti,[77a] K. Lie,[65c] J. Lieber Marin,[84e] H. Lien,[69] H. Lin,[108] K. Lin,[109] R. E. Lindley,[7] J. H. Lindon,[2] J. Ling,[62] E. Lipeles,[131] A. Lipniacka,[17] A. Lister,[167] J. D. Little,[69] B. Liu,[14] B. X. Liu,[114b] D. Liu,[63d,63c] E. H. L. Liu,[21] J. B. Liu,[63a] J. K. K. Liu,[33] K. Liu,[63d] K. Liu,[63d,63c] M. Liu,[63a] M. Y. Liu,[63a] P. Liu,[14] Q. Liu,[63d,141,63c] X. Liu,[63a] X. Liu,[63b] Y. Liu,[114b,114c] Y. L. Liu,[63b] Y. W. Liu,[63a] J. Llorente Merino,[145] S. L. Lloyd,[96] E. M. Lobodzinska,[49] P. Loch,[7] T. Lohse,[19] K. Lohwasser,[142] E. Loiacono,[49] M. Lokajicek,[134,a] J. D. Lomas,[21] J. D. Long,[165] I. Longarini,[162] R. Longo,[165] I. Lopez Paz,[68] A. Lopez Solis,[49] N. Lorenzo Martinez,[4] A. M. Lory,[111] M. Losada,[119a] G. Löschcke Centeno,[149] O. Loseva,[38] X. Lou,[48a,48b] X. Lou,[14,114c] A. Lounis,[67] P. A. Love,[93] G. Lu,[14,114c] M. Lu,[67] S. Lu,[131] Y. J. Lu,[66] H. J. Lubatti,[141] C. Luci,[76a,76b] F. L. Lucio Alves,[114a] F. Luehring,[69] I. Luise,[148] O. Lukianchuk,[67] O. Lundberg,[147] B. Lund-Jensen,[147,a] N. A. Luongo,[6] M. S. Lutz,[37] A. B. Lux,[26] D. Lynn,[30] R. Lysak,[134] E. Lytken,[100] V. Lyubushkin,[39] T. Lyubushkina,[39] M. M. Lyukova,[148] M. Firdaus M. Soberi,[53] H. Ma,[30] K. Ma,[63a] L. L. Ma,[63b] W. Ma,[63a] Y. Ma,[124] J. C. MacDonald,[102] P. C. Machado De Abreu Farias,[84e] R. Madar,[41] T. Madula,[98] J. Maeda,[86] T. Maeno,[30] H. Maguire,[142] V. Maiboroda,[138] A. Maio,[133a,133b,133d] K. Maj,[87a] O. Majersky,[49] S. Majewski,[126] N. Makovec,[67] V. Maksimovic,[16] B. Malaescu,[130] Pa. Malecki,[88] V. P. Maleev,[38] F. Malek,[61,aa] M. Mali,[95] D. Malito,[97] U. Mallik,[81] S. Maltezos,[10] S. Malyukov,[39] J. Mamuzic,[13] G. Mancini,[54] M. N. Mancini,[27] G. Manco,[74a,74b] J. P. Mandalia,[96] S. S. Mandarry,[149] I. Mandić,[95] L. Manhaes de Andrade Filho,[84a] I. M. Maniatis,[172] J. Manjarres Ramos,[91] D. C. Mankad,[172] A. Mann,[111] S. Manzoni,[37] L. Mao,[63c] X. Mapekula,[34c] A. Marantis,[155,z] G. Marchiori,[5] M. Marcisovsky,[134] C. Marcon,[72a] M. Marinescu,[21] S. Marium,[49] M. Marjanovic,[123] A. Markhoos,[55] M. Markovitch,[67] E. J. Marshall,[93] Z. Marshall,[18a] S. Marti-Garcia,[166] J. Martin,[98] T. A. Martin,[137] V. J. Martin,[53] B. Martin dit Latour,[17] L. Martinelli,[76a,76b] M. Martinez,[13,s] P. Martinez Agullo,[166] V. I. Martinez Outschoorn,[105] P. Martinez Suarez,[13]

S. Martin-Haugh,[137] G. Martinovicova,[136] V. S. Martoiu,[28b] A. C. Martyniuk,[98] A. Marzin,[37] D. Mascione,[79a,79b] L. Masetti,[102] T. Mashimo,[156] J. Masik,[103] A. L. Maslennikov,[38] P. Massarotti,[73a,73b] P. Mastrandrea,[75a,75b] A. Mastroberardino,[44b,44a] T. Masubuchi,[156] T. Mathisen,[164] J. Matousek,[136] N. Matsuzawa,[156] J. Maurer,[28b] A. J. Maury,[67] B. Maček,[95] D. A. Maximov,[38] A. E. May,[103] R. Mazini,[151] I. Maznas,[118] M. Mazza,[109] S. M. Mazza,[139] E. Mazzeo,[72a,72b] C. Mc Ginn,[30] J. P. Mc Gowan,[168] S. P. Mc Kee,[108] C. C. McCracken,[167] E. F. McDonald,[107] A. E. McDougall,[117] J. A. Mcfayden,[149] R. P. McGovern,[131] R. P. Mckenzie,[34g] T. C. Mclachlan,[49] D. J. Mclaughlin,[98] S. J. McMahon,[137] C. M. Mcpartland,[94] R. A. McPherson,[168,m] S. Mehlhase,[111] A. Mehta,[94] D. Melini,[166] B. R. Mellado Garcia,[34g] A. H. Melo,[56] F. Meloni,[49] A. M. Mendes Jacques Da Costa,[103] H. Y. Meng,[158] L. Meng,[93] S. Menke,[112] M. Mentink,[37] E. Meoni,[44b,44a] G. Mercado,[118] S. Merianos,[155] C. Merlassino,[70a,70c] L. Merola,[73a,73b] C. Meroni,[72a,72b] J. Metcalfe,[6] A. S. Mete,[6] E. Meuser,[102] C. Meyer,[69] J-P. Meyer,[138] R. P. Middleton,[137] L. Mijović,[53] G. Mikenberg,[172] M. Mikestikova,[134] M. Mikuž,[95] H. Mildner,[102] A. Milic,[37] D. W. Miller,[40] E. H. Miller,[146] L. S. Miller,[35] A. Milov,[172] D. A. Milstead,[48a,48b] T. Min,[114a] A. A. Minaenko,[38] I. A. Minashvili,[152b] L. Mince,[60] A. I. Mincer,[120] B. Mindur,[87a] M. Mineev,[39] Y. Mino,[89] L. M. Mir,[13] M. Miralles Lopez,[60] M. Mironova,[18a] A. Mishima,[156] M. C. Missio,[116] A. Mitra,[170] V. A. Mitsou,[166] Y. Mitsumori,[113] O. Miu,[158] P. S. Miyagawa,[96] T. Mkrtchyan,[64a] M. Mlinarevic,[98] T. Mlinarevic,[98] M. Mlynarikova,[37] S. Mobius,[20] P. Mogg,[111] M. H. Mohamed Farook,[115] A. F. Mohammed,[14,114c] S. Mohapatra,[42] G. Mokgatitswane,[34g] L. Moleri,[172] B. Mondal,[144] S. Mondal,[135] K. Mönig,[49] E. Monnier,[104] L. Monsonis Romero,[166] J. Montejo Berlingen,[13] A. Montella,[48a,48b] M. Montella,[122] F. Montereali,[78a,78b] F. Monticelli,[92] S. Monzani,[70a,70c] N. Morange,[67] A. L. Moreira De Carvalho,[49] M. Moreno Llácer,[166] C. Moreno Martinez,[57] P. Morettini,[58b] S. Morgenstern,[37] M. Morii,[62] M. Morinaga,[156] F. Morodei,[76a,76b] L. Morvaj,[37] P. Moschovakos,[37] B. Moser,[37] M. Mosidze,[152b] T. Moskalets,[45] P. Moskvitina,[116] J. Moss,[32,bb] P. Moszkowicz,[87a] A. Moussa,[36d] E. J. W. Moyse,[105] O. Mtintsilana,[34g] S. Muanza,[104] J. Mueller,[132] D. Muenstermann,[93] R. Müller,[37] G. A. Mullier,[164] A. J. Mullin,[33] J. J. Mullin,[131] D. P. Mungo,[158] D. Munoz Perez,[166] F. J. Munoz Sanchez,[103] M. Murin,[103] W. J. Murray,[170,137] M. Muškinja,[95] C. Mwewa,[30] A. G. Myagkov,[38,j] A. J. Myers,[8] G. Myers,[108] M. Myska,[135] B. P. Nachman,[18a] O. Nackenhorst,[50] K. Nagai,[129] K. Nagano,[85] J. L. Nagle,[30,n] E. Nagy,[104] A. M. Nairz,[37] Y. Nakahama,[85] K. Nakamura,[85] K. Nakkalil,[5] H. Nanjo,[127] E. A. Narayanan,[115] I. Naryshkin,[38] L. Nasella,[72a,72b] M. Naseri,[35] S. Nasri,[119b] C. Nass,[25] G. Navarro,[23a] J. Navarro-Gonzalez,[166] R. Nayak,[154] A. Nayaz,[19] P. Y. Nechaeva,[38] S. Nechaeva,[24b,24a] F. Nechansky,[49] L. Nedic,[129] T. J. Neep,[21] A. Negri,[74a,74b] M. Negrini,[24b] C. Nellist,[117] C. Nelson,[106] K. Nelson,[108] S. Nemecek,[134] M. Nessi,[37,cc] M. S. Neubauer,[165] F. Neuhaus,[102] J. Neundorf,[49] P. R. Newman,[21] C. W. Ng,[132] Y. W. Y. Ng,[49] B. Ngair,[119a] H. D. N. Nguyen,[110] R. B. Nickerson,[129] R. Nicolaidou,[138] J. Nielsen,[139] M. Niemeyer,[56] J. Niermann,[56] N. Nikiforou,[37] V. Nikolaenko,[38,j] I. Nikolic-Audit,[130] K. Nikolopoulos,[21] P. Nilsson,[30] I. Ninca,[49] G. Ninio,[154] A. Nisati,[76a] N. Nishu,[2] R. Nisius,[112] J-E. Nitschke,[51] E. K. Nkadimeng,[34g] T. Nobe,[156] T. Nommensen,[150] M. B. Norfolk,[142] B. J. Norman,[35] M. Noury,[36a] J. Novak,[95] T. Novak,[95] L. Novotny,[135] R. Novotny,[115] L. Nozka,[125] K. Ntekas,[162] N. M. J. Nunes De Moura Junior,[84b] J. Ocariz,[130] A. Ochi,[86] I. Ochoa,[133a] S. Oerdek,[49,dd] J. T. Offermann,[40] A. Ogrodnik,[136] A. Oh,[103] C. C. Ohm,[147] H. Oide,[85] R. Oishi,[156] M. L. Ojeda,[49] Y. Okumura,[156] L. F. Oleiro Seabra,[133a] I. Oleksiyuk,[57] S. A. Olivares Pino,[140d] G. Oliveira Correa,[13] D. Oliveira Damazio,[30] D. Oliveira Goncalves,[84a] J. L. Oliver,[162] Ö. O. Öncel,[55] A. P. O'Neill,[20] A. Onofre,[133a,133e] P. U. E. Onyisi,[11] M. J. Oreglia,[40] G. E. Orellana,[92] D. Orestano,[78a,78b] N. Orlando,[13] R. S. Orr,[158] L. M. Osojnak,[131] R. Ospanov,[63a] G. Otero y Garzon,[31] H. Otono,[90] P. S. Ott,[64a] G. J. Ottino,[18a] M. Ouchrif,[36d] F. Ould-Saada,[128] T. Ovsiannikova,[141] M. Owen,[60] R. E. Owen,[137] V. E. Ozcan,[22a] F. Ozturk,[88] N. Ozturk,[8] S. Ozturk,[83] H. A. Pacey,[129] A. Pacheco Pages,[13] C. Padilla Aranda,[13] G. Padovano,[76a,76b] S. Pagan Griso,[18a] G. Palacino,[69] A. Palazzo,[71a,71b] J. Pampel,[25] J. Pan,[175] T. Pan,[65a] D. K. Panchal,[11] C. E. Pandini,[117] J. G. Panduro Vazquez,[137] H. D. Pandya,[1] H. Pang,[15] P. Pani,[49] G. Panizzo,[70a,70c] L. Panwar,[130] L. Paolozzi,[57] S. Parajuli,[165] A. Paramonov,[6] C. Paraskevopoulos,[54] D. Paredes Hernandez,[65b] A. Pareti,[74a,74b] K. R. Park,[42] T. H. Park,[158] M. A. Parker,[33] F. Parodi,[58b,58a] E. W. Parrish,[118] V. A. Parrish,[53] J. A. Parsons,[42] U. Parzefall,[55] B. Pascual Dias,[110] L. Pascual Dominguez,[101] E. Pasqualucci,[76a] S. Passaggio,[58b] F. Pastore,[97] P. Patel,[88] U. M. Patel,[52] J. R. Pater,[103] T. Pauly,[37] C. I. Pazos,[161] J. Pearkes,[146] M. Pedersen,[128] R. Pedro,[133a]

S. V. Peleganchuk,[38] O. Penc,[37] E. A. Pender,[53] G. D. Penn,[175] K. E. Penski,[111] M. Penzin,[38] B. S. Peralva,[84d] A. P. Pereira Peixoto,[141] L. Pereira Sanchez,[146] D. V. Perepelitsa,[30,n] G. Perera,[105] E. Perez Codina,[159a] M. Perganti,[10] H. Pernegger,[37] S. Perrella,[76a,76b] O. Perrin,[41] K. Peters,[49] R. F. Y. Peters,[103] B. A. Petersen,[37] T. C. Petersen,[43] E. Petit,[104] V. Petousis,[135] C. Petridou,[155,y] T. Petru,[136] A. Petrukhin,[144] M. Pettee,[18a] A. Petukhov,[38] K. Petukhova,[37] R. Pezoa,[140f] L. Pezzotti,[37] G. Pezzullo,[175] T. M. Pham,[173] T. Pham,[107] P. W. Phillips,[137] G. Piacquadio,[148] E. Pianori,[18a] F. Piazza,[126] R. Piegaia,[31] D. Pietreanu,[28b] A. D. Pilkington,[103] M. Pinamonti,[70a,70c] J. L. Pinfold,[2] B. C. Pinheiro Pereira,[133a] A. E. Pinto Pinoargote,[138] L. Pintucci,[70a,70c] K. M. Piper,[149] A. Pirttikoski,[57] D. A. Pizzi,[35] L. Pizzimento,[65b] A. Pizzini,[117] M.-A. Pleier,[30] V. Pleskot,[136] E. Plotnikova,[39] G. Poddar,[96] R. Poettgen,[100] L. Poggioli,[130] I. Pokharel,[56] S. Polacek,[136] G. Polesello,[74a] A. Poley,[145,159a] A. Polini,[24b] C. S. Pollard,[170] Z. B. Pollock,[122] E. Pompa Pacchi,[76a,76b] N. I. Pond,[98] D. Ponomarenko,[116] L. Pontecorvo,[37] S. Popa,[28a] G. A. Popeneciu,[28d] A. Poreba,[37] D. M. Portillo Quintero,[159a] S. Pospisil,[135] M. A. Postill,[142] P. Postolache,[28c] K. Potamianos,[170] P. A. Potepa,[87a] I. N. Potrap,[39] C. J. Potter,[33] H. Potti,[150] J. Poveda,[166] M. E. Pozo Astigarraga,[37] A. Prades Ibanez,[166] J. Pretel,[55] D. Price,[103] M. Primavera,[71a] L. Primomo,[70a,70c] M. A. Principe Martin,[101] R. Privara,[125] T. Procter,[60] M. L. Proffitt,[141] N. Proklova,[131] K. Prokofiev,[65c] G. Proto,[112] J. Proudfoot,[6] M. Przybycien,[87a] W. W. Przygoda,[87b] A. Psallidas,[47] J. E. Puddefoot,[142] D. Pudzha,[55] D. Pyatiizbyantseva,[38] J. Qian,[108] D. Qichen,[103] Y. Qin,[13] T. Qiu,[53] A. Quadt,[56] M. Queitsch-Maitland,[103] G. Quetant,[57] R. P. Quinn,[167] G. Rabanal Bolanos,[62] D. Rafanoharana,[55] F. Raffaeli,[77a,77b] F. Ragusa,[72a,72b] J. L. Rainbolt,[40] J. A. Raine,[57] S. Rajagopalan,[30] E. Ramakoti,[38] I. A. Ramirez-Berend,[35] K. Ran,[49,114c] D. S. Rankin,[131] N. P. Rapheeha,[34g] H. Rasheed,[28b] V. Raskina,[130] D. F. Rassloff,[64a] A. Rastogi,[18a] S. Rave,[102] S. Ravera,[58b,58a] B. Ravina,[56] I. Ravinovich,[172] M. Raymond,[37] A. L. Read,[128] N. P. Readioff,[142] D. M. Rebuzzi,[74a,74b] G. Redlinger,[30] A. S. Reed,[112] K. Reeves,[27] J. A. Reidelsturz,[174] D. Reikher,[154] A. Rej,[50] C. Rembser,[37] M. Renda,[28b] F. Renner,[49] A. G. Rennie,[162] A. L. Rescia,[49] S. Resconi,[72a] M. Ressegotti,[58b,58a] S. Rettie,[37] J. G. Reyes Rivera,[109] E. Reynolds,[18a] O. L. Rezanova,[38] P. Reznicek,[136] H. Riani,[36d] N. Ribaric,[93] E. Ricci,[79a,79b] R. Richter,[112] S. Richter,[48a,48b] E. Richter-Was,[87b] M. Ridel,[130] S. Ridouani,[36d] P. Rieck,[120] P. Riedler,[37] E. M. Riefel,[48a,48b] J. O. Rieger,[117] M. Rijssenbeek,[148] M. Rimoldi,[37] L. Rinaldi,[24b,24a] P. Rincke,[56,164] T. T. Rinn,[30] M. P. Rinnagel,[111] G. Ripellino,[164] I. Riu,[13] J. C. Rivera Vergara,[168] F. Rizatdinova,[124] E. Rizvi,[96] B. R. Roberts,[18a] S. H. Robertson,[106,m] D. Robinson,[33] C. M. Robles Gajardo,[140f] M. Robles Manzano,[102] A. Robson,[60] A. Rocchi,[77a,77b] C. Roda,[75a,75b] S. Rodriguez Bosca,[37] Y. Rodriguez Garcia,[23a] A. Rodriguez Rodriguez,[55] A. M. Rodríguez Vera,[118] S. Roe,[37] J. T. Roemer,[37] A. R. Roepe-Gier,[139] O. Røhne,[128] R. A. Rojas,[105] C. P. A. Roland,[130] J. Roloff,[30] A. Romaniouk,[38] E. Romano,[74a,74b] M. Romano,[24b] A. C. Romero Hernandez,[165] N. Rompotis,[94] L. Roos,[130] S. Rosati,[76a] B. J. Rosser,[40] E. Rossi,[129] E. Rossi,[73a,73b] L. P. Rossi,[62] L. Rossini,[55] R. Rosten,[122] M. Rotaru,[28b] B. Rottler,[55] C. Rougier,[91] D. Rousseau,[67] D. Rousso,[49] A. Roy,[165] S. Roy-Garand,[158] A. Rozanov,[104] Z. M. A. Rozario,[60] Y. Rozen,[153] A. Rubio Jimenez,[166] A. J. Ruby,[94] V. H. Ruelas Rivera,[19] T. A. Ruggeri,[1] A. Ruggiero,[129] A. Ruiz-Martinez,[166] A. Rummler,[37] Z. Rurikova,[55] N. A. Rusakovich,[39] H. L. Russell,[168] G. Russo,[76a,76b] J. P. Rutherfoord,[7] S. Rutherford Colmenares,[33] M. Rybar,[136] E. B. Rye,[128] A. Ryzhov,[45] J. A. Sabater Iglesias,[57] P. Sabatini,[166] H. F-W. Sadrozinski,[139] F. Safai Tehrani,[76a] B. Safarzadeh Samani,[137] S. Saha,[1] M. Sahinsoy,[112] A. Saibel,[166] M. Saimpert,[138] M. Saito,[156] T. Saito,[156] A. Sala,[72a,72b] D. Salamani,[37] A. Salnikov,[146] J. Salt,[166] A. Salvador Salas,[154] D. Salvatore,[44b,44a] F. Salvatore,[149] A. Salzburger,[37] D. Sammel,[55] E. Sampson,[93] D. Sampsonidis,[155,y] D. Sampsonidou,[126] J. Sánchez,[166] V. Sanchez Sebastian,[166] H. Sandaker,[128] C. O. Sander,[49] J. A. Sandesara,[105] M. Sandhoff,[174] C. Sandoval,[23b] L. Sanfilippo,[64a] D. P. C. Sankey,[137] T. Sano,[89] A. Sansoni,[54] L. Santi,[37,76b] C. Santoni,[41] H. Santos,[133a,133b] A. Santra,[172] E. Sanzani,[24b,24a] K. A. Saoucha,[163] J. G. Saraiva,[133a,133d] J. Sardain,[7] O. Sasaki,[85] K. Sato,[160] C. Sauer,[64b] E. Sauvan,[4] P. Savard,[158,d] R. Sawada,[156] C. Sawyer,[137] L. Sawyer,[99] C. Sbarra,[24b] A. Sbrizzi,[24b,24a] T. Scanlon,[98] J. Schaarschmidt,[141] U. Schäfer,[102] A. C. Schaffer,[67,45] D. Schaile,[111] R. D. Schamberger,[148] C. Scharf,[19] M. M. Schefer,[20] V. A. Schegelsky,[38] D. Scheirich,[136] M. Schernau,[162] C. Scheulen,[56] C. Schiavi,[58b,58a] M. Schioppa,[44b,44a] B. Schlag,[146,ee] K. E. Schleicher,[55] S. Schlenker,[37] J. Schmeing,[174] M. A. Schmidt,[174] K. Schmieden,[102] C. Schmitt,[102] N. Schmitt,[102] S. Schmitt,[49] L. Schoeffel,[138] A. Schoening,[64b] P. G. Scholer,[35] E. Schopf,[129] M. Schott,[25]

J. Schovancova,[37] S. Schramm,[57] T. Schroer,[57] H-C. Schultz-Coulon,[64a] M. Schumacher,[55] B. A. Schumm,[139] Ph. Schune,[138] A. J. Schuy,[141] H. R. Schwartz,[139] A. Schwartzman,[146] T. A. Schwarz,[108] Ph. Schwemling,[138] R. Schwienhorst,[109] F. G. Sciacca,[20] A. Sciandra,[30] G. Sciolla,[27] F. Scuri,[75a] C. D. Sebastiani,[94] K. Sedlaczek,[118] S. C. Seidel,[115] A. Seiden,[139] B. D. Seidlitz,[42] C. Seitz,[49] J. M. Seixas,[84b] G. Sekhniaidze,[73a] L. Selem,[61] N. Semprini-Cesari,[24b,24a] D. Sengupta,[57] V. Senthilkumar,[166] L. Serin,[67] M. Sessa,[77a,77b] H. Severini,[123] F. Sforza,[58b,58a] A. Sfyrla,[57] Q. Sha,[14] E. Shabalina,[56] A. H. Shah,[33] R. Shaheen,[147] J. D. Shahinian,[131] D. Shaked Renous,[172] L. Y. Shan,[14] M. Shapiro,[18a] A. Sharma,[37] A. S. Sharma,[167] P. Sharma,[81] P. B. Shatalov,[38] K. Shaw,[149] S. M. Shaw,[103] Q. Shen,[63c] D. J. Sheppard,[145] P. Sherwood,[98] L. Shi,[98] X. Shi,[14] S. Shimizu,[85] C. O. Shimmin,[175] J. D. Shinner,[97] I. P. J. Shipsey,[129] S. Shirabe,[90] M. Shiyakova,[39,ff] M. J. Shochet,[40] D. R. Shope,[128] B. Shrestha,[123] S. Shrestha,[122,gg] M. J. Shroff,[168] P. Sicho,[134] A. M. Sickles,[165] E. Sideras Haddad,[34g] A. C. Sidley,[117] A. Sidoti,[24b] F. Siegert,[51] Dj. Sijacki,[16] F. Sili,[92] J. M. Silva,[53] I. Silva Ferreira,[84b] M. V. Silva Oliveira,[30] S. B. Silverstein,[48a] S. Simion,[67] R. Simoniello,[37] E. L. Simpson,[103] H. Simpson,[149] L. R. Simpson,[108] N. D. Simpson,[100] S. Simsek,[83] S. Sindhu,[56] P. Sinervo,[158] S. Singh,[158] S. Sinha,[49] S. Sinha,[103] M. Sioli,[24b,24a] I. Siral,[37] E. Sitnikova,[49] J. Sjölin,[48a,48b] A. Skaf,[56] E. Skorda,[21] P. Skubic,[123] M. Slawinska,[88] V. Smakhtin,[172] B. H. Smart,[137] S. Yu. Smirnov,[38] Y. Smirnov,[38] L. N. Smirnova,[38,j] O. Smirnova,[100] A. C. Smith,[42] D. R. Smith,[162] E. A. Smith,[40] H. A. Smith,[129] J. L. Smith,[103] R. Smith,[146] M. Smizanska,[93] K. Smolek,[135] A. A. Snesarev,[38] S. R. Snider,[158] H. L. Snoek,[117] S. Snyder,[30] R. Sobie,[168,m] A. Soffer,[154] C. A. Solans Sanchez,[37] E. Yu. Soldatov,[38] U. Soldevila,[166] A. A. Solodkov,[38] S. Solomon,[27] A. Soloshenko,[39] K. Solovieva,[55] O. V. Solovyanov,[41] P. Sommer,[37] A. Sonay,[13] W. Y. Song,[159b] A. Sopczak,[135] A. L. Sopio,[98] F. Sopkova,[29b] J. D. Sorenson,[115] I. R. Sotarriva Alvarez,[157] V. Sothilingam,[64a] O. J. Soto Sandoval,[140c,140b] S. Sottocornola,[69] R. Soualah,[163] Z. Soumaimi,[36e] D. South,[49] N. Soybelman,[172] S. Spagnolo,[71a,71b] M. Spalla,[112] D. Sperlich,[55] G. Spigo,[37] S. Spinali,[93] B. Spisso,[73a,73b] D. P. Spiteri,[60] M. Spousta,[136] E. J. Staats,[35] R. Stamen,[64a] A. Stampekis,[21] M. Standke,[25] E. Stanecka,[88] W. Stanek-Maslouska,[49] M. V. Stange,[51] B. Stanislaus,[18a] M. M. Stanitzki,[49] B. Stapf,[49] E. A. Starchenko,[38] G. H. Stark,[139] J. Stark,[91] P. Staroba,[134] P. Starovoitov,[64a] S. Stärz,[106] R. Staszewski,[88] G. Stavropoulos,[47] P. Steinberg,[30] B. Stelzer,[145,159a] H. J. Stelzer,[132] O. Stelzer-Chilton,[159a] H. Stenzel,[59] T. J. Stevenson,[149] G. A. Stewart,[37] J. R. Stewart,[124] M. C. Stockton,[37] G. Stoicea,[28b] M. Stolarski,[133a] S. Stonjek,[112] A. Straessner,[51] J. Strandberg,[147] S. Strandberg,[48a,48b] M. Stratmann,[174] M. Strauss,[123] T. Strebler,[104] P. Strizenec,[29b] R. Ströhmer,[169] D. M. Strom,[126] R. Stroynowski,[45] A. Strubig,[48a,48b] S. A. Stucci,[30] B. Stugu,[17] J. Stupak,[123] N. A. Styles,[49] D. Su,[146] S. Su,[63a] W. Su,[63d] X. Su,[63a] D. Suchy,[29a] K. Sugizaki,[156] V. V. Sulin,[38] M. J. Sullivan,[94] D. M. S. Sultan,[129] L. Sultanaliyeva,[38] S. Sultansoy,[3b] T. Sumida,[89] S. Sun,[173] O. Sunneborn Gudnadottir,[164] N. Sur,[104] M. R. Sutton,[149] H. Suzuki,[160] M. Svatos,[134] M. Swiatlowski,[159a] T. Swirski,[169] I. Sykora,[29a] M. Sykora,[136] T. Sykora,[136] D. Ta,[102] K. Tackmann,[49,dd] A. Taffard,[162] R. Tafirout,[159a] J. S. Tafoya Vargas,[67] Y. Takubo,[85] M. Talby,[104] A. A. Talyshev,[38] K. C. Tam,[65b] N. M. Tamir,[154] A. Tanaka,[156] J. Tanaka,[156] R. Tanaka,[67] M. Tanasini,[148] Z. Tao,[167] S. Tapia Araya,[140f] S. Tapprogge,[102] A. Tarek Abouelfadl Mohamed,[109] S. Tarem,[153] K. Tariq,[14] G. Tarna,[28b] G. F. Tartarelli,[72a] M. J. Tartarin,[91] P. Tas,[136] M. Tasevsky,[134] E. Tassi,[44b,44a] A. C. Tate,[165] G. Tateno,[156] Y. Tayalati,[36e,hh] G. N. Taylor,[107] W. Taylor,[159b] R. Teixeira De Lima,[146] P. Teixeira-Dias,[97] J. J. Teoh,[158] K. Terashi,[156] J. Terron,[101] S. Terzo,[13] M. Testa,[54] R. J. Teuscher,[158,m] A. Thaler,[80] O. Theiner,[57] N. Themistokleous,[53] T. Theveneaux-Pelzer,[104] O. Thielmann,[174] D. W. Thomas,[97] J. P. Thomas,[21] E. A. Thompson,[18a] P. D. Thompson,[21] E. Thomson,[131] R. E. Thornberry,[45] C. Tian,[63a] Y. Tian,[56] V. Tikhomirov,[38,j] Yu. A. Tikhonov,[38] S. Timoshenko,[38] D. Timoshyn,[136] E. X. L. Ting,[1] P. Tipton,[175] A. Tishelman-Charny,[30] S. H. Tlou,[34g] K. Todome,[157] S. Todorova-Nova,[136] S. Todt,[51] L. Toffolin,[70a,70c] M. Togawa,[85] J. Tojo,[90] S. Tokár,[29a] K. Tokushuku,[85] O. Toldaiev,[69] R. Tombs,[33] M. Tomoto,[85,113] L. Tompkins,[146,ee] K. W. Topolnicki,[87b] E. Torrence,[126] H. Torres,[91] E. Torró Pastor,[166] M. Toscani,[31] C. Tosciri,[40] M. Tost,[11] D. R. Tovey,[142] I. S. Trandafir,[28b] T. Trefzger,[169] A. Tricoli,[30] I. M. Trigger,[159a] S. Trincaz-Duvoid,[130] D. A. Trischuk,[27] B. Trocmé,[61] A. Tropina,[39] L. Truong,[34c] M. Trzebinski,[88] A. Trzupek,[88] F. Tsai,[148] M. Tsai,[108] A. Tsiamis,[155,y] P. V. Tsiareshka,[38] S. Tsigaridas,[159a] A. Tsirigotis,[155,z] V. Tsiskaridze,[158] E. G. Tskhadadze,[152a] M. Tsopoulou,[155] Y. Tsujikawa,[89] I. I. Tsukerman,[38] V. Tsulaia,[18a] S. Tsuno,[85] K. Tsuri,[121] D. Tsybychev,[148] Y. Tu,[65b] A. Tudorache,[28b]

V. Tudorache,[28b] A. N. Tuna,[62] S. Turchikhin,[58b,58a] I. Turk Cakir,[3a] R. Turra,[72a] T. Turtuvshin,[39,ii] P. M. Tuts,[42] S. Tzamarias,[155,y] E. Tzovara,[102] F. Ukegawa,[160] P. A. Ulloa Poblete,[140c,140b] E. N. Umaka,[30] G. Unal,[37] A. Undrus,[30] G. Unel,[162] J. Urban,[29b] P. Urrejola,[140a] G. Usai,[8] R. Ushioda,[157] M. Usman,[110] Z. Uysal,[83] V. Vacek,[135] B. Vachon,[106] T. Vafeiadis,[37] A. Vaitkus,[98] C. Valderanis,[111] E. Valdes Santurio,[48a,48b] M. Valente,[159a] S. Valentinetti,[24b,24a] A. Valero,[166] E. Valiente Moreno,[166] A. Vallier,[91] J. A. Valls Ferrer,[166] D. R. Van Arneman,[117] T. R. Van Daalen,[141] A. Van Der Graaf,[50] P. Van Gemmeren,[6] M. Van Rijnbach,[37] S. Van Stroud,[98] I. Van Vulpen,[117] P. Vana,[136] M. Vanadia,[77a,77b] W. Vandelli,[37] E. R. Vandewall,[124] D. Vannicola,[154] L. Vannoli,[54] R. Vari,[76a] E. W. Varnes,[7] C. Varni,[18b] T. Varol,[151] D. Varouchas,[67] L. Varriale,[166] K. E. Varvell,[150] M. E. Vasile,[28b] L. Vaslin,[85] G. A. Vasquez,[168] A. Vasyukov,[39] L. M. Vaughan,[124] R. Vavricka,[102] T. Vazquez Schroeder,[37] J. Veatch,[32] V. Vecchio,[103] M. J. Veen,[105] I. Veliscek,[30] L. M. Veloce,[158] F. Veloso,[133a,133c] S. Veneziano,[76a] A. Ventura,[71a,71b] S. Ventura Gonzalez,[138] A. Verbytskyi,[112] M. Verducci,[75a,75b] C. Vergis,[96] M. Verissimo De Araujo,[84b] W. Verkerke,[117] J. C. Vermeulen,[117] C. Vernieri,[146] M. Vessella,[105] M. C. Vetterli,[145,d] A. Vgenopoulos,[102] N. Viaux Maira,[140f] T. Vickey,[142] O. E. Vickey Boeriu,[142] G. H. A. Viehhauser,[129] L. Vigani,[64b] M. Vigl,[112] M. Villa,[24b,24a] M. Villaplana Perez,[166] E. M. Villhauer,[53] E. Vilucchi,[54] M. G. Vincter,[35] A. Visibile,[117] C. Vittori,[37] I. Vivarelli,[24b,24a] E. Voevodina,[112] F. Vogel,[111] J. C. Voigt,[51] P. Vokac,[135] Yu. Volkotrub,[87b] J. Von Ahnen,[49] E. Von Toerne,[25] B. Vormwald,[37] V. Vorobel,[136] K. Vorobev,[38] M. Vos,[166] K. Voss,[144] M. Vozak,[117] L. Vozdecky,[123] N. Vranjes,[16] M. Vranjes Milosavljevic,[16] M. Vreeswijk,[117] N. K. Vu,[63d,63c] R. Vuillermet,[37] O. Vujinovic,[102] I. Vukotic,[40] S. Wada,[160] C. Wagner,[105] J. M. Wagner,[18a] W. Wagner,[174] S. Wahdan,[174] H. Wahlberg,[92] M. Wakida,[113] J. Walder,[137] R. Walker,[111] W. Walkowiak,[144] A. Wall,[131] E. J. Wallin,[100] T. Wamorkar,[6] A. Z. Wang,[139] C. Wang,[102] C. Wang,[11] H. Wang,[18a] J. Wang,[65c] P. Wang,[98] R. Wang,[62] R. Wang,[6] S. M. Wang,[151] S. Wang,[63b] S. Wang,[14] T. Wang,[63a] W. T. Wang,[81] W. Wang,[14] X. Wang,[114a] X. Wang,[165] X. Wang,[63c] Y. Wang,[63d] Y. Wang,[114a] Y. Wang,[63a] Z. Wang,[108] Z. Wang,[63d,52,63c] Z. Wang,[108] A. Warburton,[106] R. J. Ward,[21] N. Warrack,[60] S. Waterhouse,[97] A. T. Watson,[21] H. Watson,[60] M. F. Watson,[21] E. Watton,[60,137] G. Watts,[141] B. M. Waugh,[98] J. M. Webb,[55] C. Weber,[30] H. A. Weber,[19] M. S. Weber,[20] S. M. Weber,[64a] C. Wei,[63a] Y. Wei,[55] A. R. Weidberg,[129] E. J. Weik,[120] J. Weingarten,[50] C. Weiser,[55] C. J. Wells,[49] T. Wenaus,[30] B. Wendland,[50] T. Wengler,[37] N. S. Wenke,[112] N. Wermes,[25] M. Wessels,[64a] A. M. Wharton,[93] A. S. White,[62] A. White,[8] M. J. White,[1] D. Whiteson,[162] L. Wickremasinghe,[127] W. Wiedenmann,[173] M. Wielers,[137] C. Wiglesworth,[43] D. J. Wilbern,[123] H. G. Wilkens,[37] J. J. H. Wilkinson,[33] D. M. Williams,[42] H. H. Williams,[131] S. Williams,[33] S. Willocq,[105] B. J. Wilson,[103] P. J. Windischhofer,[40] F. I. Winkel,[31] F. Winklmeier,[126] B. T. Winter,[55] J. K. Winter,[103] M. Wittgen,[146] M. Wobisch,[99] T. Wojtkowski,[61] Z. Wolffs,[117] J. Wollrath,[162] M. W. Wolter,[88] H. Wolters,[133a,133c] M. C. Wong,[139] E. L. Woodward,[42] S. D. Worm,[49] B. K. Wosiek,[88] K. W. Woźniak,[88] S. Wozniewski,[56] K. Wraight,[60] C. Wu,[21] M. Wu,[114b] M. Wu,[116] S. L. Wu,[173] X. Wu,[57] Y. Wu,[63a] Z. Wu,[4] J. Wuerzinger,[112,t] T. R. Wyatt,[103] B. M. Wynne,[53] S. Xella,[43] L. Xia,[114a] M. Xia,[15] M. Xie,[63a] S. Xin,[14,114c] A. Xiong,[126] J. Xiong,[18a] D. Xu,[14] H. Xu,[63a] L. Xu,[63a] R. Xu,[131] T. Xu,[108] Y. Xu,[15] Z. Xu,[53] Z. Xu,[114a] B. Yabsley,[150] S. Yacoob,[34a] Y. Yamaguchi,[157] E. Yamashita,[156] H. Yamauchi,[160] T. Yamazaki,[18a] Y. Yamazaki,[86] J. Yan,[63c] S. Yan,[60] Z. Yan,[105] H. J. Yang,[63c,63d] H. T. Yang,[63a] S. Yang,[63a] T. Yang,[65c] X. Yang,[37] X. Yang,[14] Y. Yang,[45] Y. Yang,[63a] Z. Yang,[63a] W-M. Yao,[18a] H. Ye,[114a] H. Ye,[56] J. Ye,[14] S. Ye,[30] X. Ye,[63a] Y. Yeh,[98] I. Yeletskikh,[39] B. K. Yeo,[18b] M. R. Yexley,[98] T. P. Yildirim,[129] P. Yin,[42] K. Yorita,[171] S. Younas,[28b] C. J. S. Young,[37] C. Young,[146] C. Yu,[14,114c] Y. Yu,[63a] J. Yuan,[14,114c] M. Yuan,[108] R. Yuan,[63d,63c] L. Yue,[98] M. Zaazoua,[63a] B. Zabinski,[88] E. Zaid,[53] Z. K. Zak,[88] T. Zakareishvili,[166] S. Zambito,[57] J. A. Zamora Saa,[140d,140b] J. Zang,[156] D. Zanzi,[55] O. Zaplatilek,[135] C. Zeitnitz,[174] H. Zeng,[14] J. C. Zeng,[165] D. T. Zenger Jr.,[27] O. Zenin,[38] T. Ženiš,[29a] S. Zenz,[96] S. Zerradi,[36a] D. Zerwas,[67] M. Zhai,[14,114c] D. F. Zhang,[142] J. Zhang,[63b] J. Zhang,[6] K. Zhang,[14,114c] L. Zhang,[63a] L. Zhang,[114a] P. Zhang,[14,114c] R. Zhang,[173] S. Zhang,[108] S. Zhang,[91] T. Zhang,[156] X. Zhang,[63c] X. Zhang,[63b] Y. Zhang,[63c] Y. Zhang,[98] Y. Zhang,[114a] Z. Zhang,[18a] Z. Zhang,[63b] Z. Zhang,[67] H. Zhao,[141] T. Zhao,[63b] Y. Zhao,[139] Z. Zhao,[63a] Z. Zhao,[63a] A. Zhemchugov,[39] J. Zheng,[114a] K. Zheng,[165] X. Zheng,[63a] Z. Zheng,[146] D. Zhong,[165] B. Zhou,[108] H. Zhou,[7] N. Zhou,[63c] Y. Zhou,[15] Y. Zhou,[114a] Y. Zhou,[7] C. G. Zhu,[63b] J. Zhu,[108] X. Zhu,[63d] Y. Zhu,[63c] Y. Zhu,[63a] X. Zhuang,[14]

K. Zhukov,[38] N. I. Zimine,[39] J. Zinsser,[64b] M. Ziolkowski,[144] L. Živković,[16] A. Zoccoli,[24b,24a] K. Zoch,[62] T. G. Zorbas,[142] O. Zormpa,[47] W. Zou,[42] and L. Zwalinski[37]

(ATLAS Collaboration)

[1]*Department of Physics, University of Adelaide, Adelaide, Australia*
[2]*Department of Physics, University of Alberta, Edmonton, Alberta, Canada*
[3a]*Department of Physics, Ankara University, Ankara, Türkiye*
[3b]*Division of Physics, TOBB University of Economics and Technology, Ankara, Türkiye*
[4]*LAPP, Université Savoie Mont Blanc, CNRS/IN2P3, Annecy, France*
[5]*APC, Université Paris Cité, CNRS/IN2P3, Paris, France*
[6]*High Energy Physics Division, Argonne National Laboratory, Argonne, Illinois, USA*
[7]*Department of Physics, University of Arizona, Tucson, Arizona, USA*
[8]*Department of Physics, University of Texas at Arlington, Arlington, Texas, USA*
[9]*Physics Department, National and Kapodistrian University of Athens, Athens, Greece*
[10]*Physics Department, National Technical University of Athens, Zografou, Greece*
[11]*Department of Physics, University of Texas at Austin, Austin, Texas, USA*
[12]*Institute of Physics, Azerbaijan Academy of Sciences, Baku, Azerbaijan*
[13]*Institut de Física d'Altes Energies (IFAE), Barcelona Institute of Science and Technology, Barcelona, Spain*
[14]*Institute of High Energy Physics, Chinese Academy of Sciences, Beijing, China*
[15]*Physics Department, Tsinghua University, Beijing, China*
[16]*Institute of Physics, University of Belgrade, Belgrade, Serbia*
[17]*Department for Physics and Technology, University of Bergen, Bergen, Norway*
[18a]*Physics Division, Lawrence Berkeley National Laboratory, Berkeley, California, USA*
[18b]*University of California, Berkeley, California, USA*
[19]*Institut für Physik, Humboldt Universität zu Berlin, Berlin, Germany*
[20]*Albert Einstein Center for Fundamental Physics and Laboratory for High Energy Physics, University of Bern, Bern, Switzerland*
[21]*School of Physics and Astronomy, University of Birmingham, Birmingham, United Kingdom*
[22a]*Department of Physics, Bogazici University, Istanbul, Türkiye*
[22b]*Department of Physics Engineering, Gaziantep University, Gaziantep, Türkiye*
[22c]*Department of Physics, Istanbul University, Istanbul, Türkiye*
[23a]*Facultad de Ciencias y Centro de Investigaciónes, Universidad Antonio Nariño, Bogotá, Colombia*
[23b]*Departamento de Física, Universidad Nacional de Colombia, Bogotá, Colombia*
[24a]*Dipartimento di Fisica e Astronomia A. Righi, Università di Bologna, Bologna, Italy*
[24b]*INFN Sezione di Bologna, Bologna, Italy*
[25]*Physikalisches Institut, Universität Bonn, Bonn, Germany*
[26]*Department of Physics, Boston University, Boston, Massachusetts, USA*
[27]*Department of Physics, Brandeis University, Waltham, Massachusetts, USA*
[28a]*Transilvania University of Brasov, Brasov, Romania*
[28b]*Horia Hulubei National Institute of Physics and Nuclear Engineering, Bucharest, Romania*
[28c]*Department of Physics, Alexandru Ioan Cuza University of Iasi, Iasi, Romania*
[28d]*National Institute for Research and Development of Isotopic and Molecular Technologies, Physics Department, Cluj-Napoca, Romania*
[28e]*National University of Science and Technology Politechnica, Bucharest, Romania*
[28f]*West University in Timisoara, Timisoara, Romania*
[28g]*Faculty of Physics, University of Bucharest, Bucharest, Romania*
[29a]*Faculty of Mathematics, Physics and Informatics, Comenius University, Bratislava, Slovak Republic*
[29b]*Department of Subnuclear Physics, Institute of Experimental Physics of the Slovak Academy of Sciences, Kosice, Slovak Republic*
[30]*Physics Department, Brookhaven National Laboratory, Upton, New York, USA*
[31]*Universidad de Buenos Aires, Facultad de Ciencias Exactas y Naturales, Departamento de Física, y CONICET, Instituto de Física de Buenos Aires (IFIBA), Buenos Aires, Argentina*
[32]*California State University, Fresno, California, USA*
[33]*Cavendish Laboratory, University of Cambridge, Cambridge, United Kingdom*
[34a]*Department of Physics, University of Cape Town, Cape Town, South Africa*
[34b]*iThemba Labs, Western Cape, South Africa*

[34c]*Department of Mechanical Engineering Science, University of Johannesburg, Johannesburg, South Africa*
[34d]*National Institute of Physics, University of the Philippines Diliman, Quezon City, Philippines*
[34e]*University of South Africa, Department of Physics, Pretoria, South Africa*
[34f]*University of Zululand, KwaDlangezwa, South Africa*
[34g]*School of Physics, University of the Witwatersrand, Johannesburg, South Africa*
[35]*Department of Physics, Carleton University, Ottawa, Ontario, Canada*
[36a]*Faculté des Sciences Ain Chock, Université Hassan II de Casablanca, Morocco*
[36b]*Faculté des Sciences, Université Ibn-Tofail, Kénitra, Morocco*
[36c]*Faculté des Sciences Semlalia, Université Cadi Ayyad, LPHEA-Marrakech, Morocco*
[36d]*LPMR, Faculté des Sciences, Université Mohamed Premier, Oujda, Morocco*
[36e]*Faculté des sciences, Université Mohammed V, Rabat, Morocco*
[36f]*Institute of Applied Physics, Mohammed VI Polytechnic University, Ben Guerir, Morocco*
[37]*CERN, Geneva, Switzerland*
[38]*Affiliated with an institute covered by a cooperation agreement with CERN*
[39]*Affiliated with an international laboratory covered by a cooperation agreement with CERN*
[40]*Enrico Fermi Institute, University of Chicago, Chicago, Illinois, USA*
[41]*LPC, Université Clermont Auvergne, CNRS/IN2P3, Clermont-Ferrand, France*
[42]*Nevis Laboratory, Columbia University, Irvington, New York, USA*
[43]*Niels Bohr Institute, University of Copenhagen, Copenhagen, Denmark*
[44a]*Dipartimento di Fisica, Università della Calabria, Rende, Italy*
[44b]*INFN Gruppo Collegato di Cosenza, Laboratori Nazionali di Frascati, Frascati, Italy*
[45]*Physics Department, Southern Methodist University, Dallas, Texas, USA*
[46]*Physics Department, University of Texas at Dallas, Richardson, Texas, USA*
[47]*National Centre for Scientific Research "Demokritos", Agia Paraskevi, Greece*
[48a]*Department of Physics, Stockholm University, Stockholm, Sweden*
[48b]*Oskar Klein Centre, Stockholm, Sweden*
[49]*Deutsches Elektronen-Synchrotron DESY, Hamburg and Zeuthen, Germany*
[50]*Fakultät Physik, Technische Universität Dortmund, Dortmund, Germany*
[51]*Institut für Kern- und Teilchenphysik, Technische Universität Dresden, Dresden, Germany*
[52]*Department of Physics, Duke University, Durham, North Carolina, USA*
[53]*SUPA—School of Physics and Astronomy, University of Edinburgh, Edinburgh, United Kingdom*
[54]*INFN e Laboratori Nazionali di Frascati, Frascati, Italy*
[55]*Physikalisches Institut, Albert-Ludwigs-Universität Freiburg, Freiburg, Germany*
[56]*II. Physikalisches Institut, Georg-August-Universität Göttingen, Göttingen, Germany*
[57]*Département de Physique Nucléaire et Corpusculaire, Université de Genève, Genève, Switzerland*
[58a]*Dipartimento di Fisica, Università di Genova, Genova, Italy*
[58b]*INFN Sezione di Genova, Genova, Italy*
[59]*II. Physikalisches Institut, Justus-Liebig-Universität Giessen, Giessen, Germany*
[60]*SUPA - School of Physics and Astronomy, University of Glasgow, Glasgow, United Kingdom*
[61]*LPSC, Université Grenoble Alpes, CNRS/IN2P3, Grenoble INP, Grenoble, France*
[62]*Laboratory for Particle Physics and Cosmology, Harvard University, Cambridge, Massachusetts, USA*
[63a]*Department of Modern Physics and State Key Laboratory of Particle Detection and Electronics, University of Science and Technology of China, Hefei, China*
[63b]*Institute of Frontier and Interdisciplinary Science and Key Laboratory of Particle Physics and Particle Irradiation (MOE), Shandong University, Qingdao, China*
[63c]*School of Physics and Astronomy, Shanghai Jiao Tong University, Key Laboratory for Particle Astrophysics and Cosmology (MOE), SKLPPC, Shanghai, China*
[63d]*Tsung-Dao Lee Institute, Shanghai, China*
[63e]*School of Physics and Microelectronics, Zhengzhou University, Zhengzhou, China*
[64a]*Kirchhoff-Institut für Physik, Ruprecht-Karls-Universität Heidelberg, Heidelberg, Germany*
[64b]*Physikalisches Institut, Ruprecht-Karls-Universität Heidelberg, Heidelberg, Germany*
[65a]*Department of Physics, Chinese University of Hong Kong, Shatin, N.T., Hong Kong, China*
[65b]*Department of Physics, University of Hong Kong, Hong Kong, China*
[65c]*Department of Physics and Institute for Advanced Study, Hong Kong University of Science and Technology, Clear Water Bay, Kowloon, Hong Kong, China*
[66]*Department of Physics, National Tsing Hua University, Hsinchu, Taiwan*
[67]*IJCLab, Université Paris-Saclay, CNRS/IN2P3, 91405, Orsay, France*
[68]*Centro Nacional de Microelectrónica (IMB-CNM-CSIC), Barcelona, Spain*
[69]*Department of Physics, Indiana University, Bloomington, Indiana, USA*

[70a]INFN Gruppo Collegato di Udine, Sezione di Trieste, Udine, Italy
[70b]ICTP, Trieste, Italy
[70c]Dipartimento Politecnico di Ingegneria e Architettura, Università di Udine, Udine, Italy
[71a]INFN Sezione di Lecce, Lecce, Italy
[71b]Dipartimento di Matematica e Fisica, Università del Salento, Lecce, Italy
[72a]INFN Sezione di Milano, Milano, Italy
[72b]Dipartimento di Fisica, Università di Milano, Milano, Italy
[73a]INFN Sezione di Napoli, Napoli, Italy
[73b]Dipartimento di Fisica, Università di Napoli, Napoli, Italy
[74a]INFN Sezione di Pavia, Pavia, Italy
[74b]Dipartimento di Fisica, Università di Pavia, Pavia, Italy
[75a]INFN Sezione di Pisa, Pisa, Italy
[75b]Dipartimento di Fisica E. Fermi, Università di Pisa, Pisa, Italy
[76a]INFN Sezione di Roma, Roma, Italy
[76b]Dipartimento di Fisica, Sapienza Università di Roma, Roma, Italy
[77a]INFN Sezione di Roma Tor Vergata, Roma, Italy
[77b]Dipartimento di Fisica, Università di Roma Tor Vergata, Roma, Italy
[78a]INFN Sezione di Roma Tre, Roma, Italy
[78b]Dipartimento di Matematica e Fisica, Università Roma Tre, Roma, Italy
[79a]INFN-TIFPA, Povo, Italy
[79b]Università degli Studi di Trento, Trento, Italy
[80]Universität Innsbruck, Department of Astro and Particle Physics, Innsbruck, Austria
[81]University of Iowa, Iowa City, Iowa, USA
[82]Department of Physics and Astronomy, Iowa State University, Ames, Iowa, USA
[83]Istinye University, Sariyer, Istanbul, Türkiye
[84a]Departamento de Engenharia Elétrica, Universidade Federal de Juiz de Fora (UFJF), Juiz de Fora, Brazil
[84b]Universidade Federal do Rio De Janeiro COPPE/EE/IF, Rio de Janeiro, Brazil
[84c]Instituto de Física, Universidade de São Paulo, São Paulo, Brazil
[84d]Rio de Janeiro State University, Rio de Janeiro, Brazil
[84e]Federal University of Bahia, Bahia, Brazil
[85]KEK, High Energy Accelerator Research Organization, Tsukuba, Japan
[86]Graduate School of Science, Kobe University, Kobe, Japan
[87a]AGH University of Krakow, Faculty of Physics and Applied Computer Science, Krakow, Poland
[87b]Marian Smoluchowski Institute of Physics, Jagiellonian University, Krakow, Poland
[88]Institute of Nuclear Physics Polish Academy of Sciences, Krakow, Poland
[89]Faculty of Science, Kyoto University, Kyoto, Japan
[90]Research Center for Advanced Particle Physics and Department of Physics, Kyushu University, Fukuoka, Japan
[91]L2IT, Université de Toulouse, CNRS/IN2P3, UPS, Toulouse, France
[92]Instituto de Física La Plata, Universidad Nacional de La Plata and CONICET, La Plata, Argentina
[93]Physics Department, Lancaster University, Lancaster, United Kingdom
[94]Oliver Lodge Laboratory, University of Liverpool, Liverpool, United Kingdom
[95]Department of Experimental Particle Physics, Jožef Stefan Institute and Department of Physics, University of Ljubljana, Ljubljana, Slovenia
[96]School of Physics and Astronomy, Queen Mary University of London, London, United Kingdom
[97]Department of Physics, Royal Holloway University of London, Egham, United Kingdom
[98]Department of Physics and Astronomy, University College London, London, United Kingdom
[99]Louisiana Tech University, Ruston, Louisiana, USA
[100]Fysiska institutionen, Lunds universitet, Lund, Sweden
[101]Departamento de Física Teorica C-15 and CIAFF, Universidad Autónoma de Madrid, Madrid, Spain
[102]Institut für Physik, Universität Mainz, Mainz, Germany
[103]School of Physics and Astronomy, University of Manchester, Manchester, United Kingdom
[104]CPPM, Aix-Marseille Université, CNRS/IN2P3, Marseille, France
[105]Department of Physics, University of Massachusetts, Amherst, Massachusetts, USA
[106]Department of Physics, McGill University, Montreal, Quebec, Canada
[107]School of Physics, University of Melbourne, Victoria, Australia
[108]Department of Physics, University of Michigan, Ann Arbor, Michigan, USA
[109]Department of Physics and Astronomy, Michigan State University, East Lansing, Michigan, USA
[110]Group of Particle Physics, University of Montreal, Montreal, Quebec, Canada

[111]*Fakultät für Physik, Ludwig-Maximilians-Universität München, München, Germany*
[112]*Max-Planck-Institut für Physik (Werner-Heisenberg-Institut), München, Germany*
[113]*Graduate School of Science and Kobayashi-Maskawa Institute, Nagoya University, Nagoya, Japan*
[114a]*Department of Physics, Nanjing University, Nanjing, China*
[114b]*School of Science, Shenzhen Campus of Sun Yat-sen University, Shenzhen, China*
[114c]*University of Chinese Academy of Science (UCAS), Beijing, China*
[115]*Department of Physics and Astronomy, University of New Mexico, Albuquerque, New Mexico, USA*
[116]*Institute for Mathematics, Astrophysics and Particle Physics, Radboud University/Nikhef, Nijmegen, Netherlands*
[117]*Nikhef National Institute for Subatomic Physics and University of Amsterdam, Amsterdam, Netherlands*
[118]*Department of Physics, Northern Illinois University, DeKalb, Illinois, USA*
[119a]*New York University Abu Dhabi, Abu Dhabi, United Arab Emirates*
[119b]*United Arab Emirates University, Al Ain, United Arab Emirates*
[120]*Department of Physics, New York University, New York, New York, USA*
[121]*Ochanomizu University, Otsuka, Bunkyo-ku, Tokyo, Japan*
[122]*The Ohio State University, Columbus, Ohio, USA*
[123]*Homer L. Dodge Department of Physics and Astronomy, University of Oklahoma, Norman, Oklahoma, USA*
[124]*Department of Physics, Oklahoma State University, Stillwater, Oklahoma, USA*
[125]*Palacký University, Joint Laboratory of Optics, Olomouc, Czech Republic*
[126]*Institute for Fundamental Science, University of Oregon, Eugene, Oregon, USA*
[127]*Graduate School of Science, Osaka University, Osaka, Japan*
[128]*Department of Physics, University of Oslo, Oslo, Norway*
[129]*Department of Physics, Oxford University, Oxford, United Kingdom*
[130]*LPNHE, Sorbonne Université, Université Paris Cité, CNRS/IN2P3, Paris, France*
[131]*Department of Physics, University of Pennsylvania, Philadelphia, Pennsylvania, USA*
[132]*Department of Physics and Astronomy, University of Pittsburgh, Pittsburgh, Pennsylvania, USA*
[133a]*Laboratório de Instrumentação e Física Experimental de Partículas—LIP, Lisboa, Portugal*
[133b]*Departamento de Física, Faculdade de Ciências, Universidade de Lisboa, Lisboa, Portugal*
[133c]*Departamento de Física, Universidade de Coimbra, Coimbra, Portugal*
[133d]*Centro de Física Nuclear da Universidade de Lisboa, Lisboa, Portugal*
[133e]*Departamento de Física, Universidade do Minho, Braga, Portugal*
[133f]*Departamento de Física Teórica y del Cosmos, Universidad de Granada, Granada (Spain), Spain*
[133g]*Departamento de Física, Instituto Superior Técnico, Universidade de Lisboa, Lisboa, Portugal*
[134]*Institute of Physics of the Czech Academy of Sciences, Prague, Czech Republic*
[135]*Czech Technical University in Prague, Prague, Czech Republic*
[136]*Charles University, Faculty of Mathematics and Physics, Prague, Czech Republic*
[137]*Particle Physics Department, Rutherford Appleton Laboratory, Didcot, United Kingdom*
[138]*IRFU, CEA, Université Paris-Saclay, Gif-sur-Yvette, France*
[139]*Santa Cruz Institute for Particle Physics, University of California Santa Cruz, Santa Cruz, California, USA*
[140a]*Departamento de Física, Pontificia Universidad Católica de Chile, Santiago, Chile*
[140b]*Millennium Institute for Subatomic physics at high energy frontier (SAPHIR), Santiago, Chile*
[140c]*Instituto de Investigación Multidisciplinario en Ciencia y Tecnología, y Departamento de Física, Universidad de La Serena, Chile*
[140d]*Universidad Andres Bello, Department of Physics, Santiago, Chile*
[140e]*Instituto de Alta Investigación, Universidad de Tarapacá, Arica, Chile*
[140f]*Departamento de Física, Universidad Técnica Federico Santa María, Valparaíso, Chile*
[141]*Department of Physics, University of Washington, Seattle, Washington, USA*
[142]*Department of Physics and Astronomy, University of Sheffield, Sheffield, United Kingdom*
[143]*Department of Physics, Shinshu University, Nagano, Japan*
[144]*Department Physik, Universität Siegen, Siegen, Germany*
[145]*Department of Physics, Simon Fraser University, Burnaby, British Columbia, Canada*
[146]*SLAC National Accelerator Laboratory, Stanford, California, USA*
[147]*Department of Physics, Royal Institute of Technology, Stockholm, Sweden*
[148]*Departments of Physics and Astronomy, Stony Brook University, Stony Brook, New York, USA*
[149]*Department of Physics and Astronomy, University of Sussex, Brighton, United Kingdom*
[150]*School of Physics, University of Sydney, Sydney, Australia*
[151]*Institute of Physics, Academia Sinica, Taipei, Taiwan*
[152a]*E. Andronikashvili Institute of Physics, Iv. Javakhishvili Tbilisi State University, Tbilisi, Georgia*

[152b]*High Energy Physics Institute, Tbilisi State University, Tbilisi, Georgia*
[152c]*University of Georgia, Tbilisi, Georgia*
[153]*Department of Physics, Technion, Israel Institute of Technology, Haifa, Israel*
[154]*Raymond and Beverly Sackler School of Physics and Astronomy, Tel Aviv University, Tel Aviv, Israel*
[155]*Department of Physics, Aristotle University of Thessaloniki, Thessaloniki, Greece*
[156]*International Center for Elementary Particle Physics and Department of Physics, University of Tokyo, Tokyo, Japan*
[157]*Department of Physics, Tokyo Institute of Technology, Tokyo, Japan*
[158]*Department of Physics, University of Toronto, Toronto, Ontario, Canada*
[159a]*TRIUMF, Vancouver, British Columbia, Canada*
[159b]*Department of Physics and Astronomy, York University, Toronto, Ontario, Canada*
[160]*Division of Physics and Tomonaga Center for the History of the Universe, Faculty of Pure and Applied Sciences, University of Tsukuba, Tsukuba, Japan*
[161]*Department of Physics and Astronomy, Tufts University, Medford, Massachusetts, USA*
[162]*Department of Physics and Astronomy, University of California Irvine, Irvine, California, USA*
[163]*University of Sharjah, Sharjah, United Arab Emirates*
[164]*Department of Physics and Astronomy, University of Uppsala, Uppsala, Sweden*
[165]*Department of Physics, University of Illinois, Urbana, Illinois, USA*
[166]*Instituto de Física Corpuscular (IFIC), Centro Mixto Universidad de Valencia—CSIC, Valencia, Spain*
[167]*Department of Physics, University of British Columbia, Vancouver, British Columbia, Canada*
[168]*Department of Physics and Astronomy, University of Victoria, Victoria, British Columbia, Canada*
[169]*Fakultät für Physik und Astronomie, Julius-Maximilians-Universität Würzburg, Würzburg, Germany*
[170]*Department of Physics, University of Warwick, Coventry, United Kingdom*
[171]*Waseda University, Tokyo, Japan*
[172]*Department of Particle Physics and Astrophysics, Weizmann Institute of Science, Rehovot, Israel*
[173]*Department of Physics, University of Wisconsin, Madison, Wisconsin, USA*
[174]*Fakultät für Mathematik und Naturwissenschaften, Fachgruppe Physik, Bergische Universität Wuppertal, Wuppertal, Germany*
[175]*Department of Physics, Yale University, New Haven, Connecticut, USA*

[a]Deceased.
[b]Also at Department of Physics, King's College London, London, United Kingdom.
[c]Also at Institute of Physics, Azerbaijan Academy of Sciences, Baku, Azerbaijan.
[d]Also at TRIUMF, Vancouver, British Columbia, Canada.
[e]Also at Department of Physics, University of Thessaly, Thessaly, Greece.
[f]Also at An-Najah National University, Nablus, Palestine.
[g]Also at Department of Physics, University of Fribourg, Fribourg, Switzerland.
[h]Also at Department of Physics, Westmont College, Santa Barbara, California, USA.
[i]Also at Departament de Fisica de la Universitat Autonoma de Barcelona, Barcelona, Spain.
[j]Also at Affiliated with an institute covered by a cooperation agreement with CERN.
[k]Also at The Collaborative Innovation Center of Quantum Matter (CICQM), Beijing, China.
[l]Also at Università di Napoli Parthenope, Napoli, Italy.
[m]Also at Institute of Particle Physics (IPP), Canada.
[n]Also at University of Colorado Boulder, Department of Physics, Boulder, Colorado, USA.
[o]Also at Borough of Manhattan Community College, City University of New York, New York, New York, USA.
[p]Also at National Institute of Physics, University of the Philippines Diliman, Diliman, Quezon City, Philippines.
[q]Also at Department of Financial and Management Engineering, University of the Aegean, Chios, Greece.
[r]Also at Centro Studi e Ricerche Enrico Fermi, Rome, Italy.
[s]Also at Institucio Catalana de Recerca i Estudis Avancats, ICREA, Barcelona, Spain.
[t]Also at Technical University of Munich, Munich, Germany.
[u]Also at CMD-AC UNEC Research Center, Azerbaijan State University of Economics (UNEC), Azerbaijan.
[v]Also at Yeditepe University, Physics Department, Istanbul, Türkiye.
[w]Also at Institute of Theoretical Physics, Ilia State University, Tbilisi, Georgia.
[x]Also at CERN, Geneva, Switzerland.
[y]Also at Center for Interdisciplinary Research and Innovation (CIRI-AUTH), Thessaloniki, Greece.
[z]Also at Hellenic Open University, Patras, Greece.
[aa]Also at Department of Physics, Stellenbosch University, South Africa.
[bb]Also at Department of Physics, California State University, Sacramento, California, USA.
[cc]Also at Département de Physique Nucléaire et Corpusculaire, Université de Genève, Genève, Switzerland.
[dd]Also at Institut für Experimentalphysik, Universität Hamburg, Hamburg, Germany.

[ee]Also at Department of Physics, Stanford University, Stanford, California, USA.
[ff]Also at Institute for Nuclear Research and Nuclear Energy (INRNE) of the Bulgarian Academy of Sciences, Sofia, Bulgaria.
[gg]Also at Washington College, Chestertown, Maryland, USA.
[hh]Also at Institute of Applied Physics, Mohammed VI Polytechnic University, Ben Guerir, Morocco.
[ii]Also at Institute of Physics and Technology, Mongolian Academy of Sciences, Ulaanbaatar, Mongolia.